HHS Public Access

Author manuscript

Dev Dyn. Author manuscript; available in PMC 2023 March 01.

Published in final edited form as:

Dev Dyn. 2022 March ; 251(3): 459–480. doi:10.1002/dvdy.416.

Early construction of the thalamocortical axon pathway requires c-Jun N-terminal kinase signaling within the ventral forebrain

Jessica G. Cunningham[1,2,3], **James D. Scripter**[1,2,3], **Stephany A. Nti**[1,3], **Eric S. Tucker**[1,3]

[1]Department of Neuroscience, West Virginia University School of Medicine, Morgantown, WV 26506

[2]Neuroscience Graduate Program, West Virginia University School of Medicine, Morgantown, WV 26506

[3]Rockefeller Neuroscience Institute, West Virginia University School of Medicine, Morgantown, WV 26506

Abstract

Background: Thalamocortical connectivity is essential for normal brain function. This important pathway is established during development, when thalamic axons extend a long distance through the forebrain before reaching the cerebral cortex. In this study, we identify a novel role for the c-Jun N-terminal Kinase (JNK) signaling pathway in guiding thalamocortical axons through intermediate target territories.

Results: Complete genetic removal of JNK signaling from the *Distal-less 5/6* (*Dlx5/6*) domain in mice prevents thalamocortical axons from crossing the diencephalon-telencephalon boundary (DTB) and the internal capsule fails to form. Ventral telencephalic cells critical for thalamocortical axon extension including corridor and guidepost neurons are also disrupted. In addition, corticothalamic, striatonigral, and nigrostriatal axons fail to cross the DTB. Analyses of different JNK mutants demonstrates that thalamocortical axon pathfinding has a non-autonomous requirement for JNK signaling.

Conclusions: We conclude that JNK signaling within the *Dlx5/6* territory enables the construction of major axonal pathways in the developing forebrain. Further exploration of this intermediate axon guidance territory is needed to uncover mechanisms of axonal pathfinding during normal brain development and to elucidate how this vital process may be compromised in neurodevelopmental disorders.

Keywords

axon guidance; intermediate target; choice point; diencephalon telencephalon boundary; corridor; guidepost cells

Correspondence: jgclemente@mix.wvu.edu.

Author Contributions

Jessica Cunningham, Conceptualization, Methodology, Formal analysis, Investigation, Writing- original draft preparation, Writing- review and editing, Visualization; James Scripter, Formal analysis, Investigation; Stephany Nti, Investigation; Eric Tucker, Conceptualization, Methodology, Supervision, Writing- review and editing, Funding acquisition.

Competing Interests

The authors declare that no competing interests exist.

Introduction

The thalamocortical pathway is a major longitudinal axon projection that connects the diencephalon to the telencephalon and functions to relay essential sensory information to the cerebral cortex [1,2]. A vital step in the formation of this connection occurs during embryonic development when growing thalamocortical axons cross the diencephalon-telencephalon boundary (DTB), an event assisted by chemorepulsion from the hypothalamus and chemoattraction to the ventral telencephalon [3]. The developing ventral telencephalon also serves as a critical intermediate target territory, containing corridor cells, guidepost neurons, and striatal axons that are necessary for proper guidance of thalamocortical axons [4–6]. The correct patterning and cellular composition of this intermediate territory is critical for establishing proper thalamocortical connectivity, as disruptions to any one of these cellular populations or their axonal projections can result in the mistargeting of thalamocortical axons [4].

The *Distal-less 5/6* (*Dlx5/6*) expression domain spans the entire axonal pathway through which thalamocortical axons project [7], including the intermediate target territory of the ventral telencephalon. Interestingly, thalamocortical axons are misrouted in mice with conditional deletions of *Linx* [8], *Ebf1* [9], *Celsr3* [10,11], or *Frizzled3* [12,13] from the *Dlx5/6* region. While these studies implicate the *Dlx5/6* territory as a critical intermediate target region for thalamocortical axons, downstream signaling pathways that could operate at the confluence of these different axon guidance systems are unknown.

The c-Jun N-terminal Kinase (JNK) signaling pathway has been implicated in axon development, including establishment of neuronal polarity, neurite architecture, axon guidance, and axon regeneration [14–19]. In mice, loss of *Jnk1* [20], the JNK scaffolding protein JIP3 [21,22], or upstream activators of JNK signaling including *DLK* [23], *MKK4* [24], and *MKK7* [25], lead to disruptions in the anterior commissure, corpus callosum, and internal capsule. The role for JNK in axon guidance within the *Dlx5/6* territory has not yet been explored, however our lab recently identified a novel role for JNK signaling in the migration of cortical interneurons arising from the *Dlx5/6* lineage [26–28]. Since the *Dlx5/6* territory instructs thalamocortical axon pathfinding and disruptions to JNK signaling alter axonal development, we sought to determine whether JNK signaling was required within *Dlx5/6* cells to establish major longitudinal axon pathways in the forebrain.

Here, we demonstrate that complete loss of JNK function from the *Dlx5/6* territory of conditional triple knockout (*cTKO*) mice results in severe thalamocortical axon misrouting from early in development. In *cTKO* mice, thalamocortical axons misroute ventrally and rostrally instead of crossing into the ventral telencephalon at the DTB. Telencephalic corridor cells are mispositioned, and guidepost cells are reduced in number. Additionally, corticothalamic, striatonigral, and nigrostriatal axons are unable to project across the DTB and thus fail to reach their intended targets. This study is the first to demonstrate a non-autonomous requirement for JNK signaling in thalamocortical axon pathfinding and establishes critical roles for JNK signaling in axons and cell populations encompassed within the *Dlx5/6* territory.

Results

Axon tracts are missing or misrouted in JNK conditional triple knockout (cTKO) mice

Genetic disruption of the *Dlx5/6*-positive forebrain territory results in severe thalamocortical and corticothalamic axonal pathfinding defects [8,10,12]. To determine whether JNK signaling is required for axon extension through this critical intermediate target territory, we utilized a conditional triple knockout (*cTKO*) mouse that conditionally removes *Jnk1* from *Dlx5/6-CRE-IRES-EGFP (Dlx5/6-CIE)* lineage cells of constitutive *Jnk2;Jnk3* double knockouts. Thus, JNK signaling is completely eliminated from the *Dlx5/6*-expressing territory through which major axon pathways traverse.

We began assessing axon tracts by labeling embryonic (E) day 17.5 brain sections with L1, a transmembrane adhesion molecule expressed by many axons in the developing brain [29]. In control brains, the internal capsule contained L1-labeled axons connecting the cortex to the thalamus (Figure 1A,E, n=3/3). In *cTKO* mice, the internal capsule was missing (Figure 1B,F, n=3/3), and instead, a large “U-shaped” bundle of ectopically positioned axons was present beneath the hypothalamus (Figure 1B, n=3/3). Commissural axon tracts including the anterior commissure and corpus callosum were present in the *cTKO* forebrain and crossed the midline (Figure 1D,F, n=3/3). However, Calbindin-labeled axons were completely absent from cTKO brains at E15.5 (Figure 1H, n=11/11).

To determine the identity of the L1-labeled axons in *cTKO* cortices, brain sections were co-labeled for L1 and Tag1, a neural adhesion molecule that marks corticofugal fibers [30] (Figure 1I–R). L1- and Tag1-positive axons were present in the intermediate zone (IZ) of both the control (Figure 1I–L; n=4/4) and *cTKO* (Figure 1N–Q; n=4/4) cortical walls at E15.5. L1-positive axons were reduced in the *cTKO* brain at the entry zone compared to controls (Figure 1M; Control: 0.057 ± 0.002 mm^2, *cTKO*: 0.048 ± 0.002 mm^2, Student’s *t*-test p=0.014, n=4), however the number of Tag1-positve axons was similar between genotypes (Figure 1R; Control: 0.045 ± 0.002 mm^2, *cTKO*: 0.045 ± 0.004 mm^2, Student’s *t*-test p=0.95, n=4). L1-positive/Tag1-negative fibers, which travel in the upper IZ, were completely absent from *cTKO* brains (Figure 1N–Q, n=4/4), suggesting that a population of axons which originated sub-cortically was affected. Thus, we identified several major axon deficiencies in *cTKO* forebrains, including a disrupted internal capsule, an ectopic accumulation of axonal fibers coursing beneath the hypothalamus, and a loss of axons normally traversing the upper IZ in the cortical wall.

Thalamocortical axons misroute ventrally in cTKO mice

Since L1-postive/Tag-1 negative axons were absent from *cTKO* cortices and there was an ectopic bundle of L1-positive axons beneath the hypothalamus, we hypothesized that thalamocortical axons were misrouted in *cTKO* brains. A DiI crystal was placed into the dorsal thalamus of fixed brain slices at E15.5 to observe the projection pattern of thalamocortical axons (Figure 2A). In control slices, DiI-labeled axons extended from the thalamus, crossed the diencephalon-telencephalon boundary (DTB), and projected through the internal capsule (Figure 2B, n=8/8). However, in *cTKO* slices, DiI-labeled axons

projected to the DTB, but rather than crossing into the telencephalon, turned ventrally into the hypothalamus (Figure 2C, n=3/3).

To further assess the trajectory of thalamocortical axons, we labeled E15.5 brain sections for NetrinG1[31]. In control brains, NetrinG1-positive thalamocortical axons crossed the DTB, extended through the internal capsule, and reached the mid-cortical wall (Figure 2D–H, n=4/4). However, in *cTKO* brains, thalamocortical axons extended from the thalamus and projected ventrally into the hypothalamus instead of crossing the DTB (Figure 2K–N, n=15/15). Additionally, a second bundle of misrouted thalamocortical axons extended rostrally in a large fascicle located at the ventromedial margin of the telencephalon in *cTKO* brains (Figure 2I–M, n=15/15). From this rostrally-projecting bundle, some thalamocortical axons splayed into the ventral forebrain at ectopic positions (Figure 2J), but with varying degrees of penetration (Figure 2N–R). In *cTKO* brains, NetrinG1-positive axons avoided entry into the ventral telencephalon completely (Figure 2O, category 1, n=6/15), entered into the telencephalon but failed to reach the internal capsule (Figure 2P, category 2, n=5/15), reached a rudimentary internal capsule but did not cross the pallial-subpallial boundary (Figure 2Q, category 3, n=2/15), or reached the cortical rudiment (Figure 2R, category 4, n=2/15), however not to the same extent as controls. Together, analyses of both DiI and NetrinG1 labeling indicate that thalamocortical axons are massively misrouted at the DTB of *cTKO* brains.

Thalamocortical and corticothalamic axons take aberrant trajectories in cTKO mice

Immunohistochemical analysis revealed that thalamocortical axons mis-projected both ventrally and rostrally in *cTKO* brains at E15.5. Despite failing to cross the DTB and properly extending through the internal capsule region, some NetrinG1-labeled thalamic projections entered the telencephalon at aberrant locations (Figure 2N–R). To determine whether these fibers eventually extended into the cortex, we examined brains at postnatal (P) day 0, the oldest age we could collect viable *cTKO* mice (Table 1). In addition, we asked whether the subcortical trajectory of cortical axons was compromised in *cTKO* mice, since thalamocortical and corticothalamic axons are known to be intimately associated with one another during development [32,33]. P0 brains were collected, fixed, hemisected along the midsagittal plane, and a DiI crystal was placed into the thalamus of one hemisphere (Figure 3A) and into the cortex of the opposite hemisphere (Figure 4A) of each brain.

In control brains, DiI-labeled axons projected from the thalamus, across the DTB, through the internal capsule, and into the cortex (Figure 3B–E; n=5/5). However, in all *cTKO* brains examined, thalamocortical axons misrouted ventrally into the hypothalamus (Figure 3H–I, L–M, n=4/4) and rostrally along the ventromedial margin of the forebrain (Figure 3F–G, J–K). Similar to the E15.5 timepoint, thalamocortical axons were observed invading the striatum from an ectopic ventral position at P0 in *cTKO* brains (Figure 3F–G, J–K). These ectopically projecting DiI-labeled fibers only reached the lateral cortex in half of the *cTKO* brains examined (Figure 3J, n=2/4) in reduced abundance compared to controls. We noticed increased ventricular volume in *cTKO* brain slices, a finding commonly reported in mouse mutants with thalamocortical axon guidance phenotypes [12,34–36]. CT scans were performed

on whole heads at P0, where we observed increased ventricular volume in the intact *cTKO* brain (Figure 3N–Q, n=6/6).

We next examined corticothalamic projections in control and *cTKO* brains (Figure 4). In control brains, DiI-labeled corticothalamic axons assumed a normal trajectory through the internal capsule, crossed into the diencephalon, and reached the dorsal thalamus (Figure 4B–D, n=5/5). Additionally, DiI-labeled cell bodies were present in the thalamus from retrograde labeling of thalamocortical axons (Figure 4D–E, n=5/5). In *cTKO* brains however, corticofugal axons were severely misrouted and did not coalesce into an organized internal capsule (Figure 4F–G,J–K, n=4/4). Instead, cortical axons ectopically entered the subpallium in large, disorganized fascicles at rostral levels (Figure 4F,J–K, n=4/4). Cortical fibers only reached the thalamus in half of the *cTKO* brains examined (Figure 4L, n=2/4). Retrogradely labeled thalamic cells were only found in *cTKO* brains that contained corticothalamic fibers in the thalamus, and when present, were reduced in number (Figure 4L–M).

Since a DiI crystal was placed into either the thalamus (Figure 3) or cortex (Figure 4) of the same hemisected brain, we compared the degree of axon misrouting between the thalamic and cortical DiI placements. Indeed, we found that in the *cTKO* brains that lacked thalamic innervation of the cortex (Figure 3F–I), no cortical axons had reached the thalamus (Figure 4F–H). Additionally, no retrogradely labeled thalamic cells were present after the cortical DiI placement (Figure 4H–I), indicating that thalamic axons had not reached the cortex in either hemisphere of each brain examined. Similarly, in *cTKO* brains with partial thalamic innervation of the cortex (Figure 3J–M), some cortical axons had reached the thalamus (Figure 4J–L), and retrogradely labeled thalamic cells were present (Figure 4L–M). Thus, reciprocal thalamocortical and corticothalamic projections were comparably affected in each hemisphere of the *cTKO* brains examined.

Thalamocortical axons are misrouted early in development in cTKO brains

We next assessed the developmental time course of thalamocortical axon misrouting in *cTKO* brains from E12.5 to P0 (Figure 5A–J). At E12.5, when thalamocortical axons first cross from the diencephalon into the telencephalon (Figure 5A inset, n=2/2), no NetrinG1-positive fibers crossed the DTB in *cTKO* mice (Figure 5F inset; n=2/2). Similarly, at E13.5 when thalamocortical axons cross the DTB (Figure 5K–L, n=6/6) and approach the pallial-subpallial boundary in control brains (Figure 5B, n=6/6), NetrinG1-positive axons were absent from the ventral telencephalon in *cTKO* mice (Figure 5G, n=8/8) and failed to cross the DTB (Figure 5M–N, n=8/8). Once misrouted, thalamocortical axons remained similarly positioned in *cTKO* brains at E15.5 (Figure 5H, n=15/15), E17.5 (Figure 5I, n=3/3), and P0 (Figure 5J, n=5/5), with the size of the “U-shaped” bundle increasing in thickness as development proceeds.

In E13.5 *cTKO* brains, thalamocortical axons extended ventrally from the thalamus and through the prethalamus (Figure 5M–N, n=8/8), suggesting their initial extension in the diencephalon is grossly unaffected, and their defect in guidance arises when challenged with crossing the DTB. Interestingly, this pathway is populated by *Dlx5/6-CIE*-positive cells and axons in control brains (Figure 5K–L, n=6/6). In *cTKO* brains however, *Dlx5/6-CIE*-positive

cells were present either in the telencephalon or diencephalon, but failed to span the DTB (Figure 5M-N, n=8/8). These data collectively suggest that thalamocortical axons are able to extend properly from the thalamus to the DTB in *cTKO* brains, however at the DTB region, there is a disruption to both thalamocortical axons and the *Dlx5/6-CIE*-positive cells and axons that normally bridge this territory.

Corridor and guidepost cells are disrupted in cTKO mice

The corridor is a permissive territory in the developing ventral telencephalon that supports the extension of thalamocortical axons through an otherwise growth inhibitory environment [5,37]. Since disruptions to the corridor region have been implicated in thalamocortical axon misrouting [4], and the *Dlx5/6* domain spans this region, we examined the corridor in control and *cTKO* brains at E13.5 (Figure 6). Brain slices were labeled for Islet1 to reveal corridor cells (Figure 6B–E), which migrate ventral-medially from the lateral ganglionic eminence (LGE) to position themselves between the Nkx2.1-positive medial ganglionic eminence (MGE) progenitor domain and the nascent globus pallidus (GP). The Islet1-positive corridor also extends caudally to the DTB, where thalamocortical axons project from the diencephalon into the telencephalon (Figure 6D–E, n=3/3). In *cTKO* brains, the overall distribution of Islet1-positive cells was similar to control brains at rostral levels (Figure 6F, n=3/3). However, immediately caudal to this location, Islet1-positive cells were ectopically positioned laterally and ventrally (Figure 6G, n=3/3). The average number of Islet1-positive cells in the corridor between the MGE and GP was not statistically different between control and *cTKO* brains (Figure 6J–K; Control: 384.0 ± 11.1, *cTKO:* 346.5 ± 21.4, Student's *t*-test p=0.19, n=3). However, there were significantly more Islet1-positive cells located ventral and lateral to the corridor in the *cTKO* brain, corresponding to the developing GP region (Figure 6J–K; Control: 217.3 ± 9.4, *cTKO:* 439.0 ± 58.0, Student's *t*-test p=0.02, n=3). At more caudal levels, where Islet1-positive cells normally associate with thalamocortical axons in control brains (Figure 6D–E, n=3/3), the Islet1-positive cells were severely reduced in number in *cTKO* brains (Figure 6L–M; Control: 923.3 ± 265.6, *cTKO*: 183.2 ± 39.4, Student's *t*-test p=0.05, n=3), and no thalamocortical axons had crossed the DTB (Figure 6H–I, n=3/3). Collectively, this suggests that Islet1-positive cells are present in the *cTKO* model, however they fail to migrate caudally and instead accumulate ectopically in rostral regions of the developing telencephalon.

Islet1-positive cells located in the telencephalon and diencephalon are critical for laying down a pioneering scaffold across the DTB for early thalamocortical axons [38]. The diencephalic Islet1-positve cells in the prethalamus are *Dlx5/6*-positive, and fail to extend across the DTB in other mouse models with thalamocortical axon defects [38]. In control brains, diencephalic Islet1-positive cells formed a scaffold beneath the thalamocortical axons (Figure 6E,O, n=3/3). Unlike telencephalic Islet1-positive cells that were depleted at this level in *cTKO* brains, diencephalic Islet1-positive cells were present in *cTKO* mice (Figure 6I,P, n=3/3) but stopped short of the DTB at the same location of the ventrally misrouted thalamocortical axons.

We next examined the Nkx2.1 expression domain, which is altered in other knockout mice with thalamocortical axon misrouting phenotypes [6,39–41]. In control brains, Nkx2.1-positive

GP cells were present throughout the corridor region and resided directly beneath the thalamocortical axons as they entered the telencephalon (Figure 6D–E, n=3/3). However, in *cTKO* brains, Nkx2.1-positive GP cells occupied a larger territory at rostral levels, extending to the lateral, pial margin of the ventral telencephalon (Figure 6F, n=3/3). Slightly more caudal, the Nkx2.1-positive GP domain shifted dorsal and lateral, in some cases splitting into multiple clusters with the apparent influx of ectopically positioned Islet1-positive cells (Figure 6G, n=3/3). Similar to Islet1-positive cells, Nkx2.1-positive cells were missing from the caudal corridor of *cTKO* brains (Figure 6H–I, n=3/3). In control brains, both Islet1-and Nkx2.1-positive cells were precisely positioned at the point of axon crossing at the DTB (Figure 6E,O, n=3/3), however, these two populations of cells failed to extend caudally to the DTB in *cTKO* brains (Figure 6I,P, n=3/3), which can be observed in both coronal and axial planes.

Another population of cells thought to assist thalamocortical axons across the DTB are guidepost cells [42], which reside in the ventral telencephalon and extend axons to the dorsal thalamus. Since these cells are often missing or reduced in number in mutants with thalamocortical axon defects [4], and are located within the *Dlx5/6* territory, we investigated whether they were present in the brains of *cTKO* mice. While the molecular profile of these guidepost cells remains unknown, they can be retrogradely labeled by placing a DiI crystal into the dorsal thalamus (Figure 7). In E13.5 control brains, thalamocortical axons crossed the DTB and projected through the ventral telencephalon (Figure 7A–B,F–G; n=6/6). Retrogradely labeled cells were found in close association with the internal capsule at both rostral (Figure 7A–B) and caudal (Figure 7F–G) levels of the ventral telencephalon in territories that were *Dlx5/6-CIE* positive. In *cTKO* brains, thalamocortical axons projected ventrally from the thalamus, but did not cross the DTB and failed to reach the telencephalon (Figure 7C–D,H–I, n=6/6). Retrogradely labeled guidepost cells were significantly reduced in number in *cTKO* brains at both rostral (Figure 7E, Control: 46.0 ± 5.0, *cTKO:* 12.3 ± 4.5, Student's *t*-test p=0.0005, n=6) and caudal (Figure 7J, Control: 20.0 ± 4.6, *cTKO:* 1.83 ± 0.70, Student's *t*-test p=0.0029, n=6) locations. Collectively, both corridor and guidepost neurons, which are known to play critical roles in early thalamocortical axon pathfinding and are present in the *Dlx5/6* domain, are disrupted in *cTKO* brains.

Reciprocal connections between the striatum and substantia nigra are altered in cTKO mice

Besides thalamocortical and corticothalamic axons, several other axonal pathways cross the DTB during early development. Two pathways in particular reciprocally connect the striatum to the substantia nigra (striatonigral) and the substantia nigra to the striatum (nigrostriatal). Since these pathways course in close proximity to thalamocortical axons as they approach the DTB, and disruptions to both the striatonigral [6,41,43] and nigrostriatal [6,44,45] pathways have been observed in mice with thalamocortical axon guidance defects, we examined striatal and nigral axon projections in *cTKO* mice (Figure 8). In control brains, Darpp32-positive striatal axons projected from the striatum, crossed the DTB, and extended to the substantia nigra in the midbrain (Figure 8A,C–E,I n=6/6). Reciprocally, tyrosine hydroxylase (TH)-positive nigral axons projected from the substantia nigra to join the median forebrain bundle, crossed the DTB, and distributed diffusely in the striatum

(Figure 8A,I n=6/6). However, in *cTKO* brains, Darpp32-positive fibers coalesced and became entangled in the striatum (Figure 8B,F; n=5/5). These striatal fibers did not cross the DTB and were therefore missing at the level of the diencephalon and substantia nigra (Figure 8B,G-H,J). TH-positive nigrostriatal fibers were likewise unable to fully extend along the anterior-posterior axis in *cTKO* brains (Figure 8B), and instead mainly misrouted in a "U-shaped" bundle into the hypothalamus (Figure 8J, n=8/8), similar to the NetrinG1-positive thalamocortical axons. In both the thalamocortical and nigrostriatal pathways, we observed similar patterns of misrouting, in which normally ipsilaterally projecting tracts were misrouted across the ventral midline. We next asked if nigrostriatal axons mis-projected early in development similar to thalamocortical axons (Figure 9). Indeed, TH-positive axons in *cTKO* mice were misrouted as early as E13.5 (Figure 9F, n=4/4), and had formed a similar "U-shaped" bundle by E15.5 (Figure 9L, n=15/15). TH-and NetrinG1-positive axons had similar patterns of misprojection from early in development, suggesting there may be a common mechanism responsible for longitudinal axon misrouting in the *cTKO* model.

Non-autonomous requirement for JNK signaling in thalamocortical axon pathfinding

Although our data strongly implicate a non-autonomous role for JNK signaling in establishing major forebrain axon tracts, we cannot exclude the possibility that the constitutive loss of *Jnk2* and *Jnk3* in *cTKO* mice impacts thalamocortical projections. At E15.5, we analyzed both the abundance of axons present in the entry zone of the cortex (Figure 10G) as well as the medial extension of axons into the cortical wall (Figure 10H). We found statistically significant alterations to TCA abundance and cortical extension between all genotypes analyzed using one-way ANOVA, and then completed post-hoc analyses using Student's *t*-tests to determine which genotypes deviated from control values. In *cTKO* mice, *Jnk1* is conditionally removed from *Dlx5/6-CIE* cells in a *Jnk2;Jnk3* double knockout background, where thalamocortical axons themselves have lost *Jnk2* and *Jnk3* function. In the *cTKO* model (Figure 10B, n=14), there are significantly fewer NetrinG1-positive axons present in the cortex at E15.5 compared to *Dlx5/6-CIE* (Figure 10A, n=6) control mice (Figure 10G; Control: 0.027 ± 0.004 mm^2, *cTKO*: 0.004 ± 0.003 mm^2, p=0.0003). The medial extension of axons into the cortex was also reduced in *cTKO* mice when compared to controls (Figure 10H; Control: 1167.0 ± 102.8 μm, *cTKO*: 58.6 ± 58.6 μm, p<0.0001). To test whether the loss of *Jnk2* and *Jnk3* alone impairs thalamocortical axon pathfinding, we developed a new mouse line to constitutively remove *Jnk2* and *Jnk3*, while leaving *Jnk1* function intact (Figure 10C, n=3). NetrinG1-positive thalamocortical axons in *Dlx5/6-CIE;Jnk2−/−;Jnk3−/−* mice extended through the internal capsule and reached the cortex at E15.5 in levels comparable to control brains (Figure 10G; *Dlx5/6-CIE;Jnk2−/−;Jnk3−/−*: 0.019 ± 0.008 mm^2, p=0.36), as well as extended a comparable distance into the cortex (Figure 10H, *Dlx5/6-CIE;Jnk2−/−;Jnk3−/−*: 1000.0 ± 134.3 μm, p=0.37). We next asked whether the removal of *Jnk1* from the *Dlx5/6* territory alone could cause thalamocortical axon misrouting (Figure 10D, n=3). In *Dlx5/6-CIE;Jnk1fl/fl* mice, where *Jnk1* is conditionally removed from the *Dlx5/6* territory but *Jnk2* and *Jnk3* remain intact, thalamocortical axons crossed the DTB and entered the cortex as normal in both the quantity of axons at the entry zone (Figure 10G; *Dlx5/6-CIE;Jnk1fl/fl*: 0.021 ± 0.004 mm^2, p=0.41) as well as the medial extension of axons into the cortex (Figure 10H; *Dlx5/6-*

CIE;Jnk1fl/fl: 973.8 ± 46.9 μm, p=0.24). Thus, the removal of *Jnk2* and *Jnk3* constitutively, or the conditional removal of only one JNK gene, *Jnk1*, from the *Dlx5/6* territory, are themselves insufficient to cause thalamocortical axon misrouting.

Since our data indicated that dosage of *JNK* gene function was an important component of the thalamocortical axon misrouting phenotype, and *JNK* genes are known to compensate for one another [46–48], we next asked whether retaining a single copy of either *Jnk1* or *Jnk3* was sufficient for proper thalamocortical axon extension. In *Dlx5/6-CIE;Jnk1fl/+;Jnk2−/−;Jnk3−/−* mice (Figure 10E, n=5), only one copy of *Jnk1* is conditionally removed from the *Dlx5/6* lineage in a *Jnk2/Jnk3* double knockout background. Thalamocortical axons were able to extend across the DTB and into the cortex of these mice at E15.5 in levels comparable to controls (Figure 10G; *Dlx5/6-CIE;Jnk1fl/+;Jnk2−/−;Jnk3−/−*: 0.026 ± 0.005 mm^2, p=0.87), suggesting that only one copy of *Jnk1* is needed in the *Dlx5/6* territory for proper thalamocortical axon extension (Figure 10H; *Dlx5/6-CIE;Jnk1fl/+;Jnk2−/−;Jnk3−/−*: 957.0 ± 38.9 μm, p=0.11). Interestingly, in *Dlx5/6-CIE;Jnk1fl/fl;Jnk2−/−;Jnk3+/−* mice (Figure 10F, n=5), where only one copy of *Jnk3* is present, thalamocortical axons were present in a similar abundance at the entry zone of the cortex when compared to controls (Figure 10G; *Dlx5/6-CIE;Jnk1fl/fl;Jnk2−/−;Jnk3+/−*: 0.026 ± 0.005 mm^2, p=0.88). However, NetrinG1-positve axons failed to extend as far medially into the cortex (Figure 10H; *Dlx5/6-CIE;Jnk1fl/fl;Jnk2−/−;Jnk3+/−*: 665.3 ± 52.2 μm, p=0.0028). When we examined all available brains from the 6 different genotypes at E15.5, we only found evidence of axon misrouting into the hypothalamus in the *cTKO* mouse. In the 5 other genotypes examined, all brains had a well-formed internal capsule, no axons misrouted at the level of the DTB, and all brains had NetrinG1-positive axons that extended into the cortex by E15.5. Although subtle axon phenotypes may exist in the other mutant genotypes (Figure 10F), our data indicate that severe axonal misrouting only occurs when JNK function is completely eliminated from the *Dlx5/6* territory.

Discussion

In the current study, we demonstrate a novel, non-autonomous requirement for JNK signaling in thalamocortical axon pathfinding. In *cTKO* mice, *Jnk1* is conditionally removed from *Dlx5/6* lineage cells in a *Jnk2/Jnk3* null background, which completely eliminates JNK signaling from the territory through which thalamocortical axons traverse. Beginning early in development, thalamocortical axons are unable to cross the diencephalon-telencephalon boundary (DTB) in *cTKO* brains, and instead misroute ventrally into the hypothalamus and rostrally along the ventromedial margin of the telencephalon. Other longitudinal axon tracts in the *cTKO* brain, including the corticothalamic, striatonigral, and nigrostriatal axons, are also unable to cross the DTB, and fail to reach their intended targets through normal trajectories. The Islet1-positive corridor and Nkx2.1-positive globus pallidus cells are mispositioned in the *cTKO* ventral telencephalon, and both fail to extend caudally to the DTB region. Guidepost cells in the ventral telencephalon which normally extend axons to the dorsal thalamus are severely reduced in number in the *cTKO* brain. An allelic series of different mouse mutants reinforced the non-autonomous requirement for JNK signaling in thalamocortical axon pathfinding and demonstrated that all three *JNK* genes must be removed from the *Dlx5/6* territory for thalamocortical axon misrouting to occur.

JNK signaling in the Dlx5/6 territory is essential for the establishment of major forebrain and midbrain axon tracts

Our data strongly suggests that correct thalamocortical axon pathfinding relies on intact JNK signaling within the *Dlx5/6* territory. The *Dlx5/6* expression domain spans much of the thalamocortical axon pathway, encompassing portions of the prethalamus and hypothalamus in the diencephalon, as well as the developing striatum, globus pallidus, and corridor region of the ventral telencephalon [7,49]. Thus, the *Dlx5/6* territory contains many axon guidance cues and intermediate target cells that normally instruct thalamocortical axon guidance, and these cells or the factors they produce may be compromised by the conditional deletion of JNK in *cTKO* mice.

For instance, crossing of the DTB by thalamocortical axons is mediated in part by chemorepulsion from the hypothalamus [50]. Hypothalamic-expressed Slits act as chemorepellents for thalamocortical axons to direct them away from the midline and steer them towards the ventral telencephalon [44,51,52]. In *Slit2* and *Slit1/Slit2* knockout mice, thalamocortical axons misroute ventrally into the hypothalamus, and in *Slit1/Slit2* knockout mice, nigrostriatal axons also ectopically project into the hypothalamus [44]. Similarly, both thalamocortical and nigrostriatal pathways misproject ventrally to form U-shaped bundles beneath the hypothalamus in *cTKO* mice. This raises the possibility that loss of JNK signaling in the *Dlx5/6* domain of the hypothalamus may compromise Slit function in the developing *cTKO* brain. Although JNK has been shown to act upstream of Slit signaling in Drosophila [53,54], connections between these pathways have not yet been identified in mice.

The *Dlx5/6*-positive ventral telencephalon contains intermediate target cells that facilitate thalamocortical axon pathfinding, including both corridor cells and guidepost neurons. Corridor cells are one population of *Dlx5/6* cells in the ventral telencephalon known to non-autonomously influence thalamocortical axon guidance. The telencephalic corridor is formed by a subset of Islet1-positive lateral ganglionic eminence cells that migrate ventromedially to form a permissive territory located between the Nkx2.1-positive medial ganglionic eminence and globus pallidus [5]. The migration of corridor cells is aided in part by Slit2 expression in the ventral telencephalon, and when disrupted, corridor cells do not migrate caudally, and thalamocortical axons fail to cross the DTB [37]. Disruption to corridor cell positioning has been reported in other mouse mutants with thalamocortical axon misrouting [5,6,37,43,55,56]. Similarly, in *cTKO* mice, which lack thalamocortical axon crossing at the DTB, both Islet1- and Nkx2.1-positive cells fail to extend caudally towards the DTB in the telencephalon, and Islet1-positive cells ectopically infiltrate the developing globus pallidus.

Guidepost neurons, which extend axons from the ventral forebrain to the dorsal thalamus, are another population of ventral telencephalic cells thought to be important in early thalamocortical axon pathfinding [42,57,58]. In *cTKO* mice, guidepost neurons, identified by retrograde labeling from the thalamus, are severely reduced in number, similar to other mutants in which thalamocortical axons fail to extend across the DTB [6,39,40,59,60]. Interestingly, guidepost neurons are *Dlx5/6*-positive, and when *Celsr3* was conditionally removed from the *Dlx5/6* territory, these cells were missing [38]. Current literature suggests that both corridor and guidepost neurons play a key role in thalamocortical axon guidance,

with disruptions to both populations of cells resulting in the misrouting of axons at the DTB. Therefore, it is likely that the loss of JNK function in the *Dlx5/6*-positive ventral telencephalon of *cTKO* brains directly disrupts both corridor and guidepost neurons, which leads to the observed non-autonomous axon misrouting phenotypes.

In addition to corridor and guidepost cells, early pioneering axons from neurons located in the ventral forebrain may assist the growth of thalamocortical axons. For instance, striatal axons have been proposed to serve as scaffolding for thalamocortical axons to cross the DTB, and indeed, in *OL-protocadherin−/−, Frizzled3−/−*, and *Celsr3−/−* mice, both striatonigral and thalamocortical axons fail to cross the DTB [6,41,43]. In *cTKO* mice, Darpp32-positive striatal axons fail to extend past the DTB, and instead coalesce in the ventral telencephalon. JNK is known to be important in neurite architecture [14], neuronal polarity [16], axon guidance [19], and axon regeneration [17], and therefore could play a role in the extension of striatal axons. Conditional removal of JNK function solely from the striatum would help determine if striatal axons have an autonomous requirement for JNK signaling, and if the striatal defects could also be responsible for axon misrouting phenotypes in *cTKO* mice.

Non-canonical WNT signaling in thalamocortical axon guidance

The Planar Cell Polarity (PCP) pathway is a component of non-canonical Wnt signaling, and is known for its roles in tissue morphogenesis, cilia organization, and directed cell migration [61,62]. Two seven-transmembrane receptors for Wnt ligands in the PCP pathway, *Frizzled3* [63,64] and *Celsr3* [65], play essential roles in axon guidance [34,35], however the underlying mechanism is currently unknown. In both *Frizzled3* and *Celsr3* knockout mice, there are severe disruptions to major axon pathways including the thalamocortical, corticothalamic, and nigrostriatal tracts, and a near complete breakdown of the internal capsule [34,35,45,66]. These findings are very reminiscent of the *cTKO* mouse, in which thalamocortical and corticothalamic axons fail to extend properly through the telencephalon, and nigrostriatal axons are misrouted at the level of the hypothalamus. *Frizzled3* and *Celsr3* have also been conditionally removed using the *Dlx5/6* driver line, and nearly identical phenotypes to the constitutive deletions of both genes have been reported [10–13], suggesting it is the expression of PCP proteins in the *Dlx5/6* territory that is critical for proper axon guidance. Interestingly, JNK signaling is thought to be a major downstream effector of the WNT/PCP pathway [67]. Thus, it is possible that PCP proteins act upstream of JNK in *Dlx5/6*-positive cells to non-autonomously regulate axon guidance in the developing forebrain.

Recent studies have looked more closely at the intermediate target territories in both the *Celsr3* and *Frizzied3* mutants. Ventral telencephalic guidepost cells were missing or severely reduced in *Celsr3* [41] and *Dlx5/6;Celsr3fl/fl* [38] mice, respectively, similar to the severe reduction observed in the *cTKO* forebrain. In *cTKO* mice, telencephalic Islet1-positive corridor cells invade the globus pallidus, which was also observed in *Celsr3* [41] and *Frizzled3* [43] mutants. *Islet1*-positive cells in the prethalamus, another *Dlx5/6*-positive domain, fail to extend across the DTB in *cTKO* and *Islet1Cre;Celsr3fl/fl* mice [38]. Additionally, in both the *Celsr3* and *cTKO* mutants, Nkx2.1-positive cells failed to extend caudally to the DTB region [41]. Finally, striatal connections were compromised in both *Celsr3−/−* and *Frizzled3−/−* mice

[41,43], similar to Darpp32-positive axons failing to extend past the DTB in *cTKO* brains. While mechanisms underlying the interplay between intermediate target cells and growing axons from major pathways in the developing forebrain remain to be fully dissected, it will be important to determine whether JNK acts downstream of non-canonical WNT signaling to coordinate this process.

Conclusions

Thalamocortical axons extend a long distance to reach their cortical targets, and disruptions at any point along their trajectory can lead to lasting changes in neural connectivity and function. Here, we identified a novel, non-autonomous requirement for JNK signaling in the early pathfinding of thalamocortical axons. Elucidation of upstream and downstream regulators of JNK function in this critical developmental process will advance our understanding of thalamocortical connectivity, and in turn, inform us on how neurodevelopmental diseases may arise.

Experimental Procedures

Animals

The Office of Laboratory Animal Resources at West Virginia University housed and cared for mice (*Mus musculus*) used in these studies. All mouse procedures were approved by and performed in accordance with the Institutional Animal Care and Use Committee at West Virginia University. Mice in all crosses were acquired and maintained on a C57BL/6J background. The individual mouse strains are as follows: C57BL/6J (Stock # 000664, The Jackson Laboratory); *Dlx5/6*-Cre-IRES-EGFP (*Dlx5/6-CIE*; [49], floxed Mapk8tm1Rjd mice Jnk1fl/fl; [68]; kindly provided by Dr. Roger Davis); Mapk9tm1Flv (*Jnk2−/−;* Stock # 004321, The Jackson Laboratory); Mapk10tm1Flv (*Jnk3−/−;* Stock # 004322, The Jackson Laboratory). *Dlx5/6-CIE* control animals were generated by crossing C57BL/6J dams with *Dlx5/6-CIE* hemizygous males. *Jnk1fl/fl;Jnk2−/−;Jnk3−/−* dams were mated with *Dlx5/6-CIE;Jnk1fl/+;Jnk2−/−;Jnk3+/−* males to generate *Dlx5/6-CIE;Jnk1fl/fl;Jnk2−/−;Jnk3−/−*), *Dlx5/6-CIE;Jnk1fl/+;Jnk2−/−;Jnk3−/−*, and *Dlx5/6-CIE;Jnk1fl/fl;Jnk2−/−;Jnk3+/−* mice. *Jnk2+/−;Jnk3−/−* dams were mated with *Dlx5/6-CIE;Jnk2−/−;Jnk3+/−* males to generate *Dlx5/6-CIE;Jnk2−/−;Jnk3−/−* animals. *Jnk1f/fl* dams were mated with *Dlx5/6-CIE;Jnk1fl/+* males to generate *Dlx5/6-CIE;Jnk1fl/fl* animals.

Tissue collection and processing

Dams were placed into male cages each night and checked every morning for a vaginal plug. The day of the vaginal plug was recorded as embryonic day 0.5. Timed-pregnant dams were euthanized, embryos were collected in 1X phosphate-buffered saline (PBS; 136.9mmol NaCl, 2.683mmol KCl, 4.290mmol Na_2HP0_4 $7H_2O$, 1.470mmol KH_2P0_4), and tissue was taken for genotyping. E12.5 and E13.5 whole heads were submerged in 4% paraformaldehyde in PBS (PFA; Millipore Sigma, 818715). E15.5 and E17.5 brains were dissected, then submerged in 4% PFA. For P0 collections, newborn pups were deeply anesthetized and transcardially perfused with 1X PBS followed by 4% PFA. P0 brains were dissected and submerged in 4% PFA. All material was fixed for 24 hours in 4% PFA at

4°C before being passaged through a sucrose series (10%, 20%, 30%) for cryoprotection. Material was then embedded in Tissue Freezing Medium (VWR 15146-019), frozen, and stored at −80°C. Frozen material was sectioned at 12 μm on a Leica cryostat (CM3050S) onto superfrost plus slides (Fisher, 12-550-15), and stored at −20°C prior to staining.

Immunohistochemistry and imaging

Slides were outlined with a pap pen (Electron Microscopy Sciences, 71310), and rehydrated for 20 mins with 1X PBS, followed by blocking buffer containing permeabilization solution [26] with either 5% normal donkey (EMD Millipore, S30-100ml) or goat serum (Thermofisher scientific, 16210064). Primary antibody was diluted in block, placed on the slides, and incubated overnight at 4°C. Slides were then rinsed with 1X PBS, followed by incubation with secondary antibodies diluted in block for 2 hours at room temperature. After incubation, slides were rinsed again with 1X PBS and counterstained with Hoechst (Thermo Scientific 62249, 1μg/ml) for 10 minutes. Slides were rinsed before being cover-slipped with mounting media (Mowiol 4-88, Polysciences, 17951) containing an anti-fade reagent (p-Phenylenediamine, Fisher Scientific, AC130570050). All slides were stored at 4°C prior to imaging. Brain sections were imaged using an Olympus VS120 Slide Scanner with a UPLSAPO 10x objective, as well as on a Zeiss 710 confocal microscope with a 20x Plan-Apo objective lens.

Primary Antibodies:

Host:	Antigen:	Concentration:	Company:	Product Number:
Rabbit	Calbindin	1:2000	Swant	CB38
Rabbit	Darpp-32	1:1000	Synaptic Systems	382 002
Chicken	GFP	1:1500	Abcam	ab13970
Goat	Islet1	1:500	R&D Systems	AF1837
Rabbit	L1	1:250	Aviva Systems Biology	ARP63103
Goat	NetrinG1	1:250	R&D Systems	AF1166
Rabbit	Nkx2.1	1:500	Santa Cruz	sc-13040
Rabbit	p-JNK	1:1000	Promega	V7931
Mouse	Tag1	1:12.5	DSHB	AB_2315433
Chicken	TH	1:1000	Aves Labs	TYH

Secondary Antibodies:

Antibody:	Concentration:	Company:	Product Number:
Donkey anti-Chicken 488	1:4000	Jackson Immuno Research	703-545-155
Goat anti-Chicken 488	1:4000	Invitrogen	A11039
Donkey anti-Goat 546	1:2000	Invitrogen	A11056
Goat anti-Chicken 546	1:2000	Invitrogen	A11040
Goat anti-Mouse 546	1:2000	Invitrogen	A11003
Goat anti-Rabbit 546	1:2000	Invitrogen	A11010

Antibody:	Concentration:	Company:	Product Number:
Donkey anti-Chicken 647	1:2000	Jackson Immuno Research	703-605-155
Donkey anti-Rabbit 647	1:2000	Jackson Immuno Research	711-605-152
Goat anti-Rabbit 647	1:2000	Invitrogen	A21244

Analyses of immunohistochemically-labeled slices

E13.5.—Serially sectioned brains labeled with Islet1 were imaged on the Slide Scanner. For each brain (n=3/genotype), two sections from the rostral portion of the corridor and two sections from the caudal portion of the corridor region were used for analysis. At the rostral position, Islet1-positive cells were counted in the corridor region between the MGE and GP, as well as in a portion of the ventral forebrain located ventrolateral to the corridor, which included the GP itself. At the caudal position, Islet1-positive cells in the ventral forebrain were counted at the DTB. Overall statistical significance was determined using Student's *t*-tests.

E15.5 axon abundance.—Coronal brain sections labeled with Tag1, L1, and NetrinG1 were imaged on the Slide Scanner. For each brain, three coronal sections were used for the Tag1/L1 analysis (n=4/genotype), and four coronal sections were used for the NetrinG1 analysis (minimum of n=3/genotype). A defined region at the entry zone of the cortex was cropped, and the Tag1, L1, or NetrinG1 signal within each cropped image was masked and the area of labeled fibers was measured using Nikon Elements Imaging Software Version 5.02. Overall statistical significance between control and *cTKO* genotypes was determined using Student's *t*-tests for the Tag1 and L1 analyses, and by using one-way ANOVA followed by post-hoc Student's *t*-tests for the multi-genotype comparison in the NetrinG1 analysis.

E15.5 axon extension into the cortex.—For each brain (minimum of n=3/genotype), four coronal sections labeled for NetrinG1 were analyzed. The distance between the entry zone of the cortex and the medial most extension of NetrinG1-positive axons into the cortex was measured in each brain section in Adobe Photoshop Version 20.0.7. Overall statistical significance between genotypes was determined using one-way ANOVA followed by post-hoc Student's *t*-tests.

DiI labeling

E13.5.—Dissected heads from E13.5 embryos were fixed in 4% PFA overnight at 4°C. Following fixation, heads were rinsed into 1X PBS. Whole heads were hemi-sected along the mid-sagittal plane, and a DiI crystal (Invitrogen, D3911) was placed into the dorsal thalamus of both halves of the brain. DiI-labeled heads were incubated at 37°C for 2 weeks in the dark in 1X PBS. Following incubation, each hemi-sected head was embedded in 3% agarose (Fisher Scientific, BP165-25), sectioned in the coronal plane at 150 μm on a Leica vibratome (VT1000S), and slide mounted in series. Two slices from each brain were used for quantification of retrogradely-labeled cells in the ventral telencephalon. The section in which thalamocortical axons were at the diencephalon-telencephalon boundary region was

selected as the caudal position, and the slice immediately rostral to this location was used as the rostral position. The total number of DiI-positive cells located within the ventral telencephalon of each slice were counted in both the rostral and caudal positions in n=6 brains per genotype, and overall statistical differences were determined by Student's *t*-tests.

E15.5.—E15.5 brains were fixed in 1.5% PFA overnight at 4°C. After rinsing into 1X PBS, brains were embedded in 3% agarose and then sectioned coronally at 300 μm on a vibratome. DiI crystals were placed into one half of the dorsal thalamus in each of the slices. DiI-labeled brain slices were incubated for 3 days at room temperature in 1X PBS in the dark before being mounted onto slides.

P0.—P0 mice were perfused and brains were stored in 4% PFA for 1 week at 4°C. Brains were then rinsed into 1X PBS and hemi-sected along the mid-sagittal plane. DiI crystals were placed into the thalamus of the right hemisphere, and into the cortex of the left hemisphere. DiI-labeled brains were incubated at 37°C for 8 weeks in the dark. Each half of the brain was embedded in 3% agarose, sectioned at 200 μm on a vibratome, then slide mounted before imaging. DiI-labeled brains from all timepoints were imaged with a Zeiss 710 confocal microscope using a 20x Plan-Apo objective lens.

CT scans

P0 mice were perfused and heads were fixed in 4% PFA for 2 days at 4°C, after which they were transferred to stability buffer (4% w/v paraformaldehyde (pH 7.2), 4% w/v acrylamide (Bio-Rad 1610140), 0.05% w/v bis-acrylamide (Bio-Rad 1610142), 0.25% w/v VA044 initiator (Fisher Scientific, NC0632395), 0.05% w/v Saponin (EMD Millipore, 558255), in 1x PBS) for 3 days at 4°C [69]. The samples underwent nitrogen desiccation in stability buffer (3 minutes vacuum, 3 minutes Nitrogen, 3 minutes vacuum), and then were placed in a water bath at 37°C for 3 hours. Heads were carefully removed from the stability buffer and placed in 0.1 N iodine (Thermo Fisher Scientific, AC12422) to stain for 2 days, with iodine being replaced at 24 hours. The heads were embedded in 3% agarose, then were imaged on a Bruker SkyScan 1272 MicroCT scanner (Al 0.5 mm filter, 850 ms exposure, and 7 μm resolution).

Acknowledgements

We would like to thank Amanda Ammer and Karen Martin for their excellent microscopy assistance. Imaging was performed in the WVU Imaging Facilities, which have been supported by the WVU Cancer Institute, the WVU HSC Office of Research and Graduate Education, and NIH grants P20RR016440, P30GM103488, U54GM104942, P20GM103434, and P30GM103503. This work was partially supported by a transition grant from the Office of Research and Graduate Education at WVU Health Sciences Center (EST) and graduate stipend support from NIH grant T32 GM133369 (JDS).

Funding

This work was funded by the National Institutes of Health grant R01NS082262 to E.S.T.

Grant Sponsor and Grant Number:

This work was funded by the National Institutes of Health grant R01NS082262 to Eric S. Tucker.

References

1. Leyva-Diaz E, Lopez-Bendito G. In and out from the cortex: development of major forebrain connections. Neuroscience. Dec 19 2013;254:26–44. 10.1016/j.neuroscience.2013.08.070. [PubMed: 24042037]
2. Jones EG. The thalamic matrix and thalamocortical synchrony. Trends Neurosci. Oct 2001;24(10):595–601. 10.1016/s0166-2236(00)01922-6. [PubMed: 11576674]
3. Lopez-Bendito G, Molnar Z. Thalamocortical development: how are we going to get there? Nat Rev Neurosci. Apr 2003;4(4):276–89. 10.1038/nrn1075. [PubMed: 12671644]
4. Molnar Z, Garel S, Lopez-Bendito G, Maness P, Price DJ. Mechanisms controlling the guidance of thalamocortical axons through the embryonic forebrain. Eur J Neurosci. May 2012;35(10):1573–85. 10.1111/j.1460-9568.2012.08119.x. [PubMed: 22607003]
5. Lopez-Bendito G, Cautinat A, Sanchez JA, et al. Tangential neuronal migration controls axon guidance: a role for neuregulin-1 in thalamocortical axon navigation. Cell. Apr 7 2006;125(1):127–42. 10.1016/j.cell.2006.01.042. [PubMed: 16615895]
6. Uemura M, Nakao S, Suzuki ST, Takeichi M, Hirano S. OL-Protocadherin is essential for growth of striatal axons and thalamocortical projections. Nat Neurosci. Sep 2007;10(9):1151–9. 10.1038/nn1960. [PubMed: 17721516]
7. Panganiban G, Rubenstein JL. Developmental functions of the Distal-less/Dlx homeobox genes. Development. Oct 2002;129(19):4371–86. [PubMed: 12223397]
8. Mandai K, Reimert DV, Ginty DD. Linx mediates interaxonal interactions and formation of the internal capsule. Neuron. Jul 2 2014;83(1):93–103. 10.1016/j.neuron.2014.05.020. [PubMed: 24930700]
9. Lokmane L, Proville R, Narboux-Nême N, et al. Sensory Map Transfer to the Neocortex Relies on Pretarget Ordering of Thalamic Axons. Current biology. 05/06/2013 2013;23(9). 10.1016/j.cub.2013.03.062.
10. Zhou L, Bar I, Achouri Y, et al. Early forebrain wiring: genetic dissection using conditional Celsr3 mutant mice. Science. May 16 2008;320(5878):946–9. 10.1126/science.1155244. [PubMed: 18487195]
11. Zhou L, Qu Y, Tissir F, Goffinet AM. Role of the atypical cadherin Celsr3 during development of the internal capsule. Cereb Cortex. Jul 2009; 19 Suppl 1:i114–9. 10.1093/cercor/bhp032. [PubMed: 19349379]
12. Hua ZL, Jeon S, Caterina MJ, Nathans J. Frizzled3 is required for the development of multiple axon tracts in the mouse central nervous system. Proc Natl Acad Sci U S A. Jul 22 2014;111(29):E3005–14. 10.1073/pnas.1406399111. [PubMed: 24799694]
13. Qu Y, Huang Y, Feng J, et al. Genetic evidence that Celsr3 and Celsr2, together with Fzd3, regulate forebrain wiring in a Vangl-independent manner. Proc Natl Acad Sci U S A. Vol 111. 2014:E2996–3004. [PubMed: 25002511]
14. Coffey ET, Hongisto V, Dickens M, Davis RJ, Courtney MJ. Dual Roles for c-Jun N-Terminal Kinase in Developmental and Stress Responses in Cerebellar Granule Neurons. J Neurosci. Vol 20. 2000:7602–13. [PubMed: 11027220]
15. Tararuk T, Ostman N, Li W, et al. JNK1 phosphorylation of SCG10 determines microtubule dynamics and axodendritic length. J Cell Biol. Apr 24 2006;173(2):265–77. 10.1083/jcb.200511055. [PubMed: 16618812]
16. Oliva AA Jr., Atkins CM, Copenagle L, Banker GA. Activated c-Jun N-terminal kinase is required for axon formation. J Neurosci. Sep 13 2006;26(37):9462–70. 10.1523/jneurosci.2625-06.2006. [PubMed: 16971530]
17. Raivich G, Bohatschek M, Da Costa C, et al. The AP-1 transcription factor c-Jun is required for efficient axonal regeneration. Neuron. Jul 8 2004;43(1):57–67. 10.1016/j.neuron.2004.06.005. [PubMed: 15233917]
18. Schellino R, Boido M, Vercelli A. JNK Signaling Pathway Invovlement in Spinal Cord Neuron Development and Death. Cells. 2019; Dec; 8(12): 1576.

19. Shafer B, Onishi K, Lo C, Colakoglu G, Zou Y. Vangl2 promotes Wnt/planar cell polarity-like signaling by antagonizing Dvl1-mediated feedback inhibition in growth cone guidance. Developmental cell. 02/15/2011 2011;20(2). 10.1016/j.devcel.2011.01.002.
20. Chang L, Jones Y, Ellisman MH, Goldstein LS, Karin M. JNK1 is required for maintenance of neuronal microtubules and controls phosphorylation of microtubule-associated proteins. Dev Cell. Apr 2003;4(4):521–33. [PubMed: 12689591]
21. Kelkar N, Delmotte MH, Weston CR, et al. Morphogenesis of the telencephalic commissure requires scaffold protein JNK-interacting protein 3 (JIP3). Proc Natl Acad Sci U S A. Aug 19 2003;100(17):9843–8. 10.1073/pnas.1733944100. [PubMed: 12897243]
22. Cho IH, Lee KW, Ha HY, Han PL. JNK/stress-activated protein kinase associated protein 1 is required for early development of telencephalic commissures in embryonic brains. Exp Mol Med. Aug 31 2011;43(8):462–70. 10.3858/emm.2011.43.8.052. [PubMed: 21685723]
23. Hirai S, Cui DF, Miyata T, et al. The c-Jun N-terminal kinase activator dual leucine zipper kinase regulates axon growth and neuronal migration in the developing cerebral cortex. J Neurosci. Nov 15 2006;26(46):11992–2002. 10.1523/jneurosci.2272-06.2006. [PubMed: 17108173]
24. Wang X, Nadarajah B, Robinson AC, et al. Targeted deletion of the mitogen-activated protein kinase kinase 4 gene in the nervous system causes severe brain developmental defects and premature death. Mol Cell Biol. Nov 2007;27(22):7935–46. 10.1128/mcb.00226-07. [PubMed: 17875933]
25. Yamasaki T, Kawasaki H, Arakawa S, et al. Stress-activated protein kinase MKK7 regulates axon elongation in the developing cerebral cortex. J Neurosci. Nov 16 2011;31(46):16872–83. 10.1523/jneurosci.1111-11.2011. [PubMed: 22090513]
26. Myers AK, Meechan DW, Adney DR, Tucker ES. Cortical interneurons require Jnk1 to enter and navigate the developing cerebral cortex. J Neurosci. Jun 4 2014;34(23):7787–801. 10.1523/jneurosci.4695-13.2014. [PubMed: 24899703]
27. Myers AK, Cunningham JG, Smith SE, Snow JP, Smoot CA, Tucker ES. JNK signaling is required for proper tangential migration and laminar allocation of cortical interneurons. Development. Jan 17 2020;147(2). 10.1242/dev.180646.
28. Smith S, Coker N, Tucker E. JNK Signaling Regulates Cellular Mechanics of Cortical Interneuron Migration. eNeuro. 08/20/2020 2020;7,4(4). 10.1523/ENEURO.0132-20.2020.
29. Stallcup WB, Beasley LL, Levine JM. Antibody against nerve growth factor-inducible large external (NILE) glycoprotein labels nerve fiber tracts in the developing rat nervous system. J Neurosci. Apr 1985;5(4):1090–101. [PubMed: 3981244]
30. Wolfer DP, Henehan-Beatty A, Stoeckli ET, Sonderegger P, Lipp HP. Distribution of TAG-1/axonin-1 in fibre tracts and migratory streams of the developing mouse nervous system. J Comp Neurol. Jul 1 1994;345(1):1–32. 10.1002/cne.903450102. [PubMed: 8089271]
31. Nakashiba T, Ikeda T, Nishimura S, et al. Netrin-G1: a novel glycosyl phosphatidylinositol-linked mammalian netrin that is functionally divergent from classical netrins. J Neurosci. Sep 1 2000;20(17):6540–50. [PubMed: 10964959]
32. Molnar Z, Adams R, Blakemore C. Mechanisms underlying the early establishment of thalamocortical connections in the rat. J Neurosci. Aug 1 1998;18(15):5723–45. [PubMed: 9671663]
33. Chen Y, Magnani D, Theil T, Pratt T, Price DJ. Evidence that descending cortical axons are essential for thalamocortical axons to cross the pallial-subpallial boundary in the embryonic forebrain. PLoS One. 2012;7(3):e33105. 10.1371/journal.pone.0033105. [PubMed: 22412988]
34. Wang Y, Thekdi N, Smallwood PM, Macke JP, Nathans J. Frizzled-3 is required for the development of major fiber tracts in the rostral CNS. J Neurosci. Oct 1 2002;22(19):8563–73. [PubMed: 12351730]
35. Tissir F, Bar I, Jossin Y, De Backer O, Goffinet AM. Protocadherin Celsr3 is crucial in axonal tract development. Nat Neurosci. Apr 2005;8(4):451–7. 10.1038/nn1428. [PubMed: 15778712]
36. Hua ZL, Emiliani FE, Nathans J. Rac1 plays an essential role in axon growth and guidance and in neuronal survival in the central and peripheral nervous systems. Neural Dev. Sep 23 2015;10:21. 10.1186/s13064-015-0049-3. [PubMed: 26395878]

37. Bielle F, Marcos-Mondejar P, Keita M, et al. Slit2 activity in the migration of guidepost neurons shapes thalamic projections during development and evolution. Neuron. Mar 24 2011;69(6):1085–98. 10.1016/j.neuron.2011.02.026. [PubMed: 21435555]
38. Feng J, Xian Q, Guan T, et al. Celsr3 and Fzd3 Organize a Pioneer Neuron Scaffold to Steer Growing Thalamocortical Axons. Cereb Cortex. Jul 2016;26(7):3323–34. 10.1093/cercor/bhw132. [PubMed: 27170656]
39. Tuttle R, Nakagawa Y, Johnson JE, O'Leary DD. Defects in thalamocortical axon pathfinding correlate with altered cell domains in Mash-1-deficient mice. Development. May 1999;126(9):1903–16. [PubMed: 10101124]
40. Lakhina V, Falnikar A, Bhatnagar L, Tole S. Early thalamocortical tract guidance and topographic sorting of thalamic projections requires LIM-homeodomain gene Lhx2. Dev Biol. Jun 15 2007;306(2):703–13. 10.1016/j.ydbio.2007.04.007. [PubMed: 17493606]
41. Jia Z, Guo Y, Tang Y, Xu Q, Li B, Wu Q. Regulation of the protocadherin Celsr3 gene and its role in globus pallidus development and connectivity. Mol Cell Biol. Oct 2014;34(20):3895–910. 10.1128/mcb.00760-14. [PubMed: 25113559]
42. Braisted JE, Tuttle R, O'Leary DD. Thalamocortical axons are influenced by chemorepellent and chemoattractant activities localized to decision points along their path. Dev Biol. Apr 15 1999;208(2):430–40. 10.1006/dbio.1999.9216. [PubMed: 10191056]
43. Morello F, Prasad AA, Rehberg K, et al. Frizzled3 Controls Axonal Polarity and Intermediate Target Entry during Striatal Pathway Development. J Neurosci. Oct 21 2015;35(42):14205–19. 10.1523/jneurosci.1840-15.2015. [PubMed: 26490861]
44. Bagri A, Marin O, Plump AS, et al. Slit proteins prevent midline crossing and determine the dorsoventral position of major axonal pathways in the mammalian forebrain. Neuron. Jan 17 2002;33(2):233–48. [PubMed: 11804571]
45. Fenstermaker AG, Prasad AA, Bechara A, et al. Wnt/planar cell polarity signaling controls the anterior-posterior organization of monoaminergic axons in the brainstem. J Neurosci. Nov 24 2010;30(47):16053–64. 10.1523/jneurosci.4508-10.2010. [PubMed: 21106844]
46. Brecht S, Kirchhof R, Chromik A, et al. Specific pathophysiological functions of JNK isoforms in the brain. Eur J Neurosci. Jan 2005;21(2):363–77. 10.1111/j.1460-9568.2005.03857.x. [PubMed: 15673436]
47. Chen JT, Lu DH, Chia CP, Ruan DY, Sabapathy K, Xiao ZC. Impaired long-term potentiation in c-Jun N-terminal kinase 2-deficient mice. J Neurochem. Apr 2005;93(2):463–73. 10.1111/j.1471-4159.2005.03037.x. [PubMed: 15816869]
48. Jaeschke A, Karasarides M, Ventura JJ, et al. JNK2 is a positive regulator of the cJun transcription factor. Mol Cell. Sep 15 2006;23(6):899–911. 10.1016/j.molcel.2006.07.028. [PubMed: 16973441]
49. Stenman J, Toresson H, Campbell K. Identification of two distinct progenitor populations in the lateral ganglionic eminence: implications for striatal and olfactory bulb neurogenesis. J Neurosci. Jan 1 2003;23(1):167–74. [PubMed: 12514213]
50. Anton-Bolanos N, Espinosa A, Lopez-Bendito G. Developmental interactions between thalamus and cortex: a true love reciprocal story. Curr Opin Neurobiol. Oct 2018;52:33–41. 10.1016/j.conb.2018.04.018. [PubMed: 29704748]
51. Braisted JE, Ringstedt T, O'Leary DD. Slits are chemorepellents endogenous to hypothalamus and steer thalamocortical axons into ventral telencephalon. Cereb Cortex. Jul 2009;19 Suppl 1:i144–51. 10.1093/cercor/bhp035. [PubMed: 19435711]
52. Lopez-Bendito G, Flames N, Ma L, et al. Robo1 and Robo2 cooperate to control the guidance of major axonal tracts in the mammalian forebrain. J Neurosci. Mar 28 2007;27(13):3395–407. 10.1523/jneurosci4605-06.2007. [PubMed: 17392456]
53. Vaughen J, Igaki T. Slit-Robo Repulsive Signaling Extrudes Tumorigenic Cells from Epithelia. Dev Cell. Dec 19 2016;39(6):683–695. 10.1016/j.devcel.2016.11.015. [PubMed: 27997825]
54. Iida C, Ohsawa S, Taniguchi K, Yamamoto M, Morata G, Igaki T. JNK-mediated Slit-Robo signaling facilitates epithelial wound repair by extruding dying cells. Sci Rep. Dec 20 2019;9(1):19549. 10.1038/s41598-019-56137-z. [PubMed: 31863086]

55. Simpson TI, Pratt T, Mason JO, Price DJ. Normal ventral telencephalic expression of Pax6 is required for normal development of thalamocortical axons in embryonic mice. Neural Dev. Jun 5 2009;4:19. 10.1186/1749-8104-4-19. [PubMed: 19500363]
56. Backer S, Lokmane L, Landragin C, Deck M, Garel S, Bloch-Gallego E. Trio GEF mediates RhoA activation downstream of Slit2 and coordinates telencephalic wiring. Development. Oct 2 2018;145(19). 10.1242/dev.153692.
57. Metin C, Godement P. The ganglionic eminence may be an intermediate target for corticofugal and thalamocortical axons. J Neurosci. May 15 1996;16(10):3219–35. [PubMed: 8627360]
58. Molnar Z, Cordery P. Connections between cells of the internal capsule, thalamus, and cerebral cortex in embryonic rat. J Comp Neurol. Oct 11 1999;413(1):1–25. [PubMed: 10464367]
59. Jones L, Lopez-Bendito G, Gruss P, Stoykova A, Molnar Z. Pax6 is required for the normal development of the forebrain axonal connections. Development. Nov 2002;129(21):5041–52. [PubMed: 12397112]
60. Mitsogiannis MD, Little GE, Mitchell KJ. Semaphorin-Plexin signaling influences early ventral telencephalic development and thalamocortical axon guidance. Neural Dev. Apr 24 2017;12(1):6. 10.1186/s13064-017-0083-4. [PubMed: 28438183]
61. Wang Y, Nathans J. Tissue/planar cell polarity in vertebrates: new insights and new questions. Development. Feb 2007;134(4):647–58. 10.1242/dev.02772. [PubMed: 17259302]
62. Simons M, Mlodzik M. Planar cell polarity signaling: from fly development to human disease. Annu Rev Genet. 2008;42:517–40. 10.1146/annurev.genet.42.110807.091432. [PubMed: 18710302]
63. Vinson CR, Conover S, Adler PN. A Drosophila tissue polarity locus encodes a protein containing seven potential transmembrane domains. Nature. Mar 16 1989;338(6212):263–4. 10.1038/338263a0. [PubMed: 2493583]
64. Goodrich LV, Strutt D. Principles of planar polarity in animal development. Development. May 2011;138(10):1877–92. 10.1242/dev.054080. [PubMed: 21521735]
65. Usui T, Shima Y, Shimada Y, et al. Flamingo, a seven-pass transmembrane cadherin, regulates planar cell polarity under the control of Frizzled. Cell. Sep 3 1999;98(5):585–95. 10.1016/s0092-8674(00)80046-x. [PubMed: 10490098]
66. Wang Y, Zhang J, Mori S, Nathans J. Axonal growth and guidance defects in Frizzled3 knock-out mice: a comparison of diffusion tensor magnetic resonance imaging, neurofilament staining, and genetically directed cell labeling. J Neurosci. Jan 11 2006;26(2):355–64. 10.1523/jneurosci.3221-05.2006. [PubMed: 16407530]
67. Niehrs C The complex world of WNT receptor signalling. Nat Rev Mol Cell Biol. Dec 2012;13(12):767–79. 10.1038/nrm3470. [PubMed: 23151663]
68. Das M, Jiang F, Sluss HK, et al. Suppression of p53-dependent senescence by the JNK signal transduction pathway. Proc Natl Acad Sci U S A. Oct 2 2007;104(40):15759–64. 10.1073/pnas.0707782104. [PubMed: 17893331]
69. Hsu CW, Wong L, Rasmussen TL, et al. Three-dimensional microCT imaging of mouse development from early post-implantation to early postnatal stages. Dev Biol. Nov 15 2016;419(2):229–236. 10.1016/j.ydbio.2016.09.011. [PubMed: 27671873]

Key Findings:

- Thalamocortical axons misroute at the diencephalic-telencephalic boundary (DTB) in mice lacking JNK signaling in *Distal-less 5/6*-positive cells of the ventral forebrain.
- Intermediate targets of thalamocortical axon guidance including corridor cells, striatal axons, and ventral telencephalic guidepost neurons are disrupted in these mice.
- Corticothalamic, striatonigral, and nigrostriatal axon pathways are also misrouted and fail to cross the DTB in these mice.

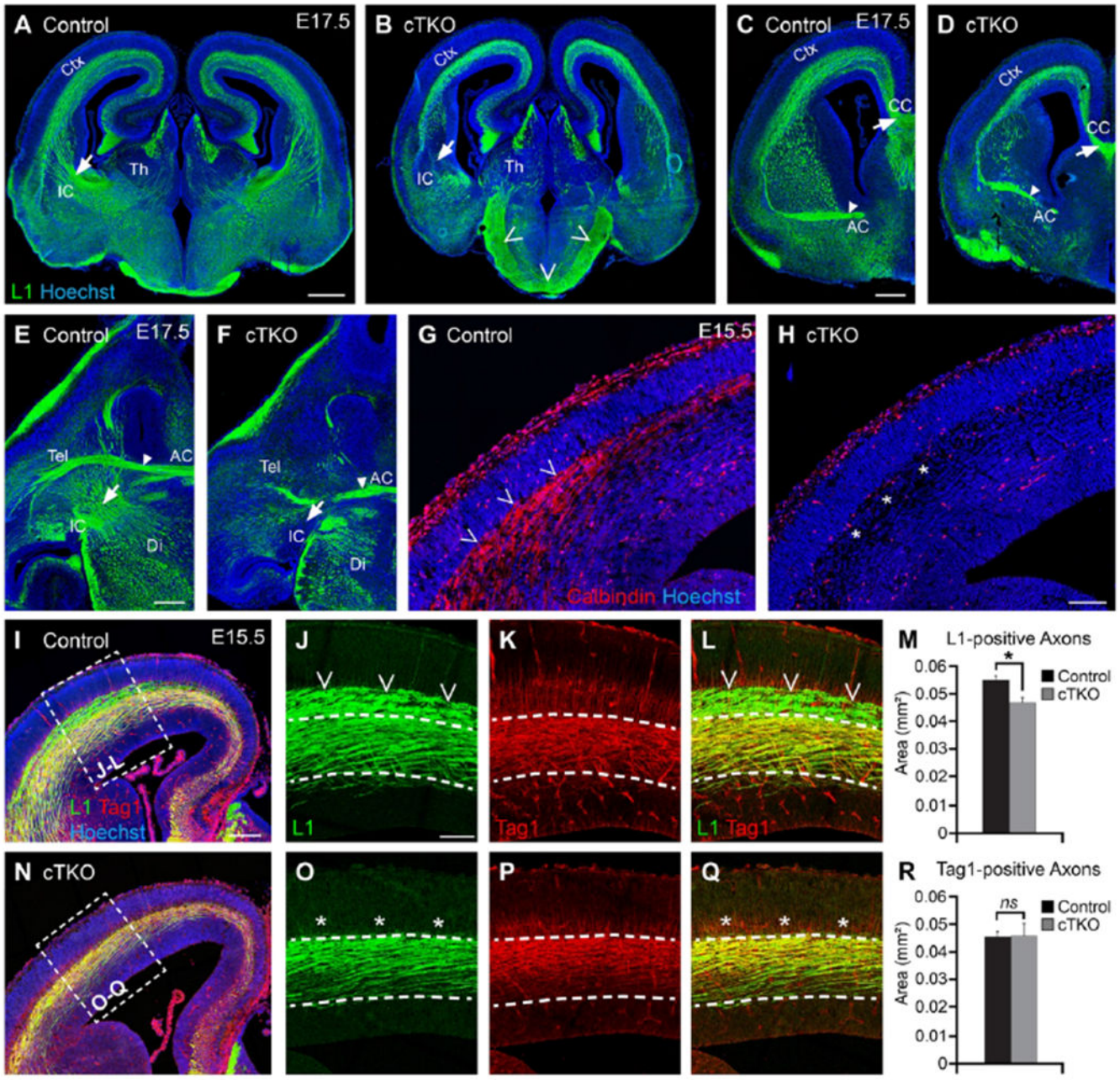

Figure 1. Subsets of axon tracts are missing or misrouted in the *cTKO* brain.

A-F. L1 labeling in coronal (A-D) and axial (E-F) sections of E17.5 brains. The internal capsule (arrow) is present in control (A,E) but not *cTKO* (B,F) brains. An ectopic "U-shaped" bundle projects into the hypothalamus of *cTKO* brains (open arrowheads, B). The corpus callosum (arrows) and anterior commissure (closed arrowheads) both cross the midline in control (C,E) and *cTKO* (D,F) brains. G-H. Immunohistochemistry for calbindin in E15.5 brain sections labels a population of axons in the cortical wall of control brains (open arrowheads, G), which are missing from *cTKO* cortices (asterisks, H). I-R. E15.5 cortices labeled with L1 and Tag1. L1- and Tag1-positive axons are present in control (I-L)

and *cTKO* (N-Q) cortices. L1-positive axons are reduced in *cTKO* cortices (M), however Tag1-positve axons are similar between genotypes (R). A population of L1-positive/Tag1-negative axons is present in control brains (open arrowheads, J-L), but missing in *cTKO* brains (asterisks, O-Q). AC- anterior commissure, Ctx- cortex, CC- corpus callosum, IC- internal capsule, Ththalamus, Tel- telencephalon, Di- diencephalon. Scale bars: A-B 500 μm; C-F 300 μm; G,H 100 μm; I,N 200 μm; J-L,O-Q 100 μm.

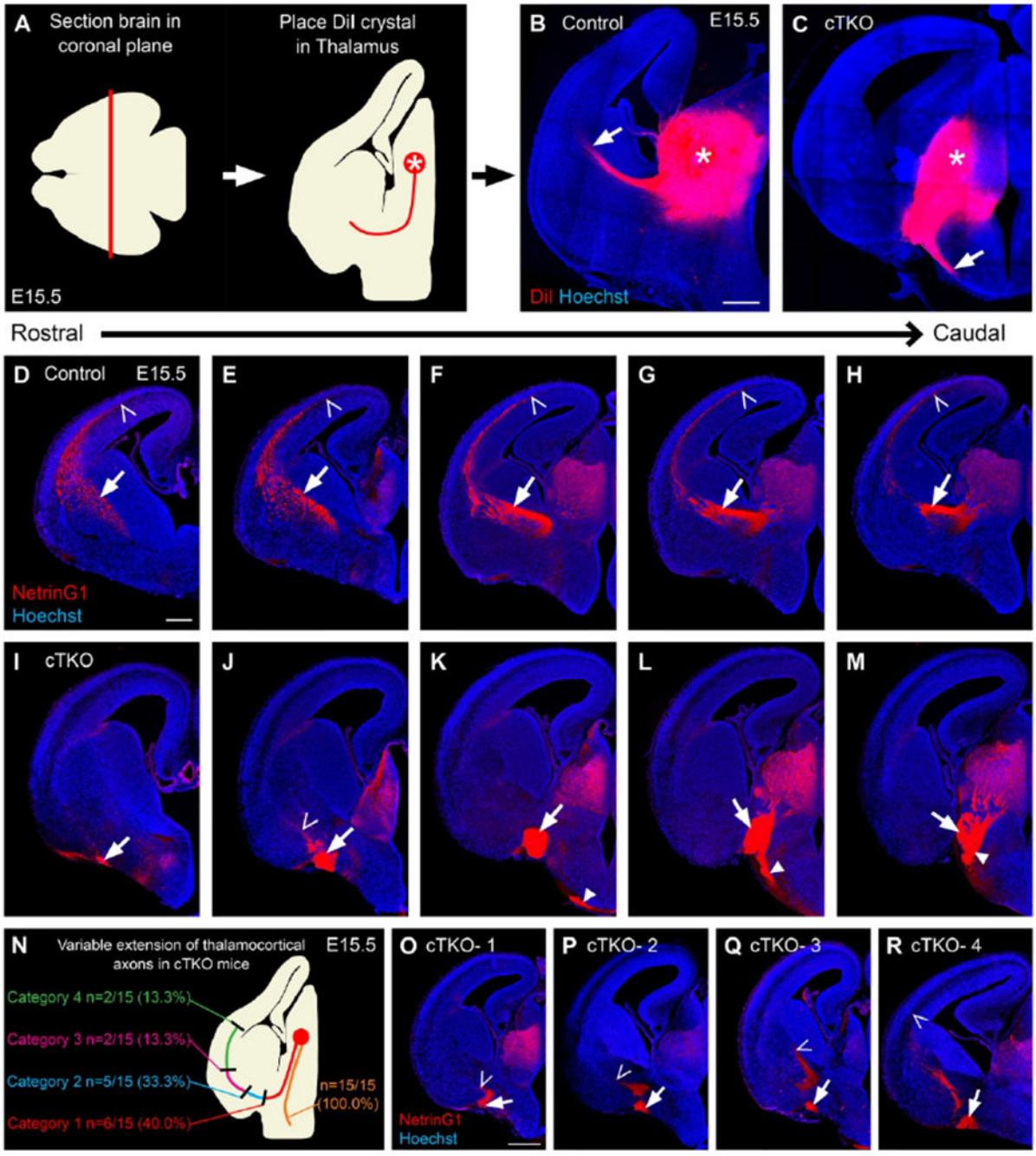

Figure 2. Thalamocortical axons are misrouted in *cTKO* brains.

A. E15.5 brains were fixed, sectioned coronally at 300 μm, and a DiI crystal (asterisk) was placed into the dorsal thalamus. B-C. DiI labels axons projecting through the internal capsule of control brains (arrow, B), and axons projecting ventrally into the hypothalamus of *cTKO* brains (arrow, C). D-M. NetrinG1-labeled thalamocortical axons in rostrocaudal series of control (D-H) and *cTKO* (I-M) brains at E15.5. In control brains, axons project through the internal capsule (arrow, D-H) and reach the cortex at all levels (open arrowheads, D-H). In *cTKO* brains, fibers aberrantly project ventrally into the hypothalamus

(closed arrowheads, K-M), rostrally along the ventromedial margin of the telencephalon (arrows, I-M), and into the striatum at ectopic locations (open arrowhead, J). N-R. 15 *cTKO* brains were stained with NetrinG1 along the rostrocaudal axis at E15.5. NetrinG1-positive axons aberrantly projected into the hypothalamus in all 15 *cTKO* brains. Some *cTKO* brains contained NetrinG1 fibers that entered the telencephalon, but the degree that these fibers penetrated was variable (categories 1-4). Scale bars: B-M 300 μm, O-R 200 μm.

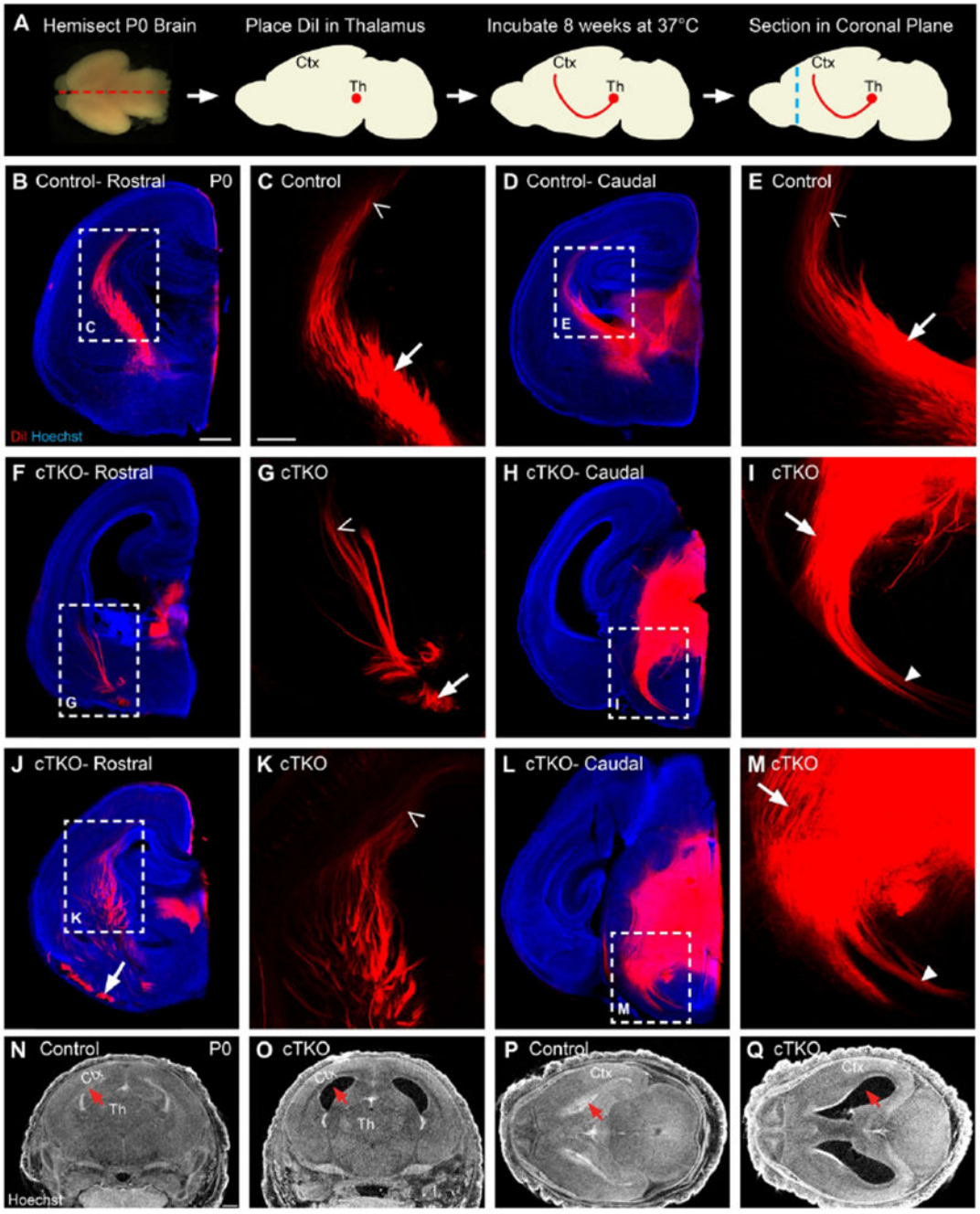

Figure 3. Axons projecting from the thalamus have aberrant trajectories in the P0 *cTKO* brain.

A. P0 brains were hemisected, DiI-labeled in the thalamus, incubated, and coronally sectioned at 200 μm. B-E. DiI-labeled axons in control brains project through the internal capsule (arrow) to reach the cortex (open arrowhead) at rostral (B, C) and caudal (D, E) locations. F-M. DiI-labeled axons in *cTKO* brains project ventrally at caudal locations (arrow, I,M) and extend into the hypothalamus (closed arrowhead, I,M). At more rostral levels (F-G, J-K), a bundle of axons resides along the ventral margin of the telencephalon (arrow, G,J). DiI-labeled axons in some *cTKO* brains stop in the striatum (open arrowhead,

G), while DiI-labeled axons in other *cTKO* brains reach the cortex (open arrowhead, K) in reduced numbers. N-Q. CT images of whole heads at P0 in coronal (N,O) and axial (P,Q) views demonstrate enlarged ventricles (red arrows) in *cTKO* brains (O,Q). Ctx- cortex, Th- thalamus. Scale bars: B,D,F,H,J,L 500 μm; C,E,G,I,K,M 200 μm; N-Q 800 μm.

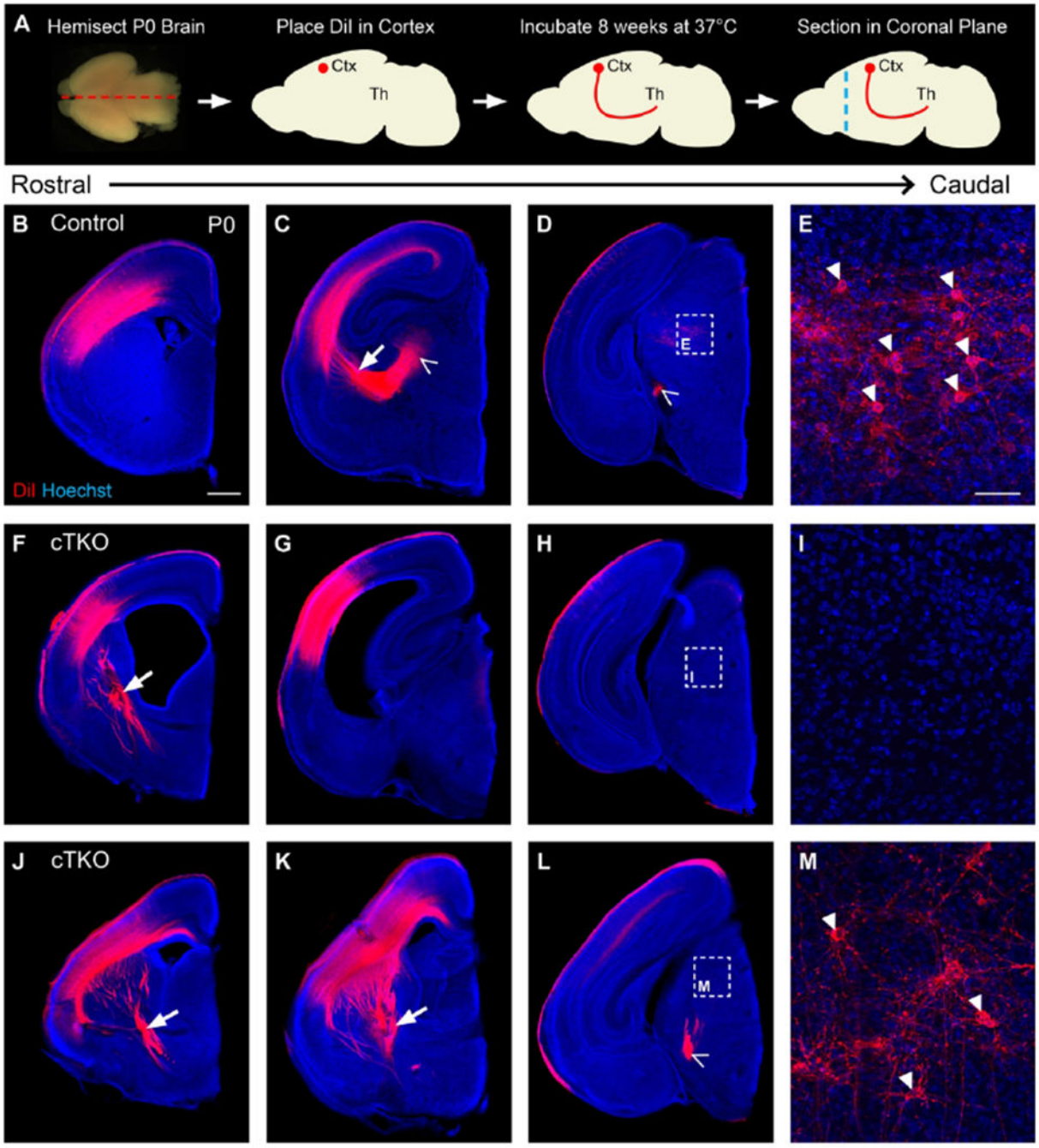

Figure 4. Corticothalamic axons display aberrant projection patterns in the P0 *cTKO* brain.

A. P0 brains were hemisected, DiI-labeled in the cortex, incubated, and coronally sectioned at 200 μm. B-E. DiI-labeled cortical axons in control brains project through the internal capsule (arrow, C) and into the thalamus (open arrowheads, C-D). Cell bodies of retrogradely labeled thalamocortical neurons are present in the thalamus (closed arrowheads, E). F-M. DiI-labeled cortical axons in *cTKO* brains project rostrally and ventrally in large torturous fascicles (arrows, F,J-K). In n = 2/4 cTKO brains (F-I), no cortical axons reach the thalamus (G-H), and no retrogradely labeled cells are present (I). In n = 2/4 *cTKO* brains

(J-M), axons reach the thalamus (open arrowhead, L), and retrogradely labeled cells are present (closed arrowheads, M). Scale bars: B-D, F-H, J-L 500 μm; E,I,M 50 μm.

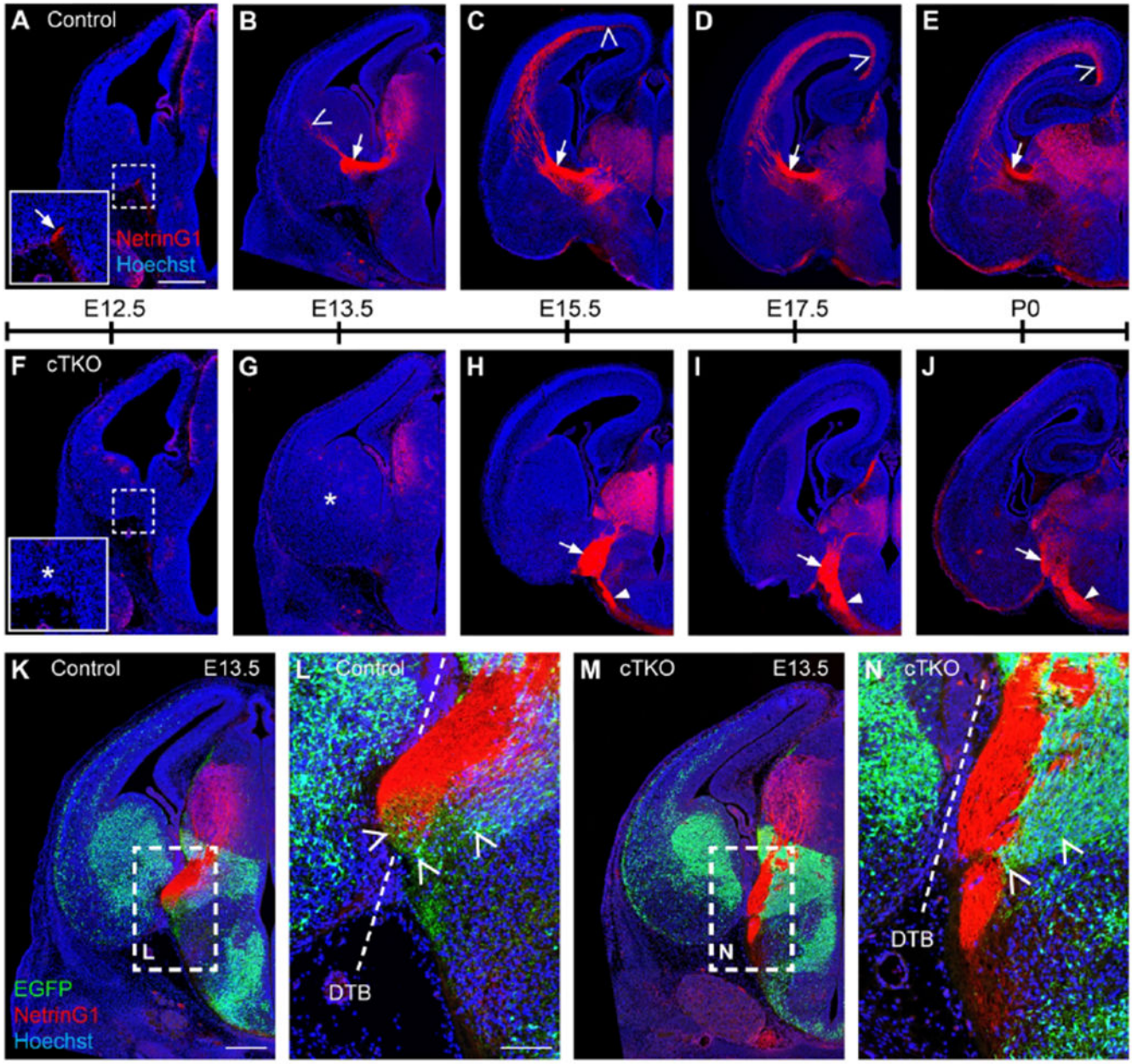

Figure 5. Thalamocortical axons are misrouted from early developmental timepoints in the *cTKO* brain.

A-E. NetrinG1 labeling of thalamocortical axons from E12.5 to P0 in control brains at the level of the diencephalon-telencephalon boundary (DTB). Axons extend into the ventral telencephalon at E12.5 (arrow-inset, A), reach the pallial-subpallial boundary at E13.5 (open arrowhead, B), and continue to extend through the internal capsule (arrows, B-E) and into the cortex from E15.5-P0 (open arrowheads, C-E). F-G. In *cTKO* brains, NetrinG1-positive axons are missing in the ventral telencephalon at E12.5 (asterisk, F) and E13.5 (asterisk, G). H-J. Axons are present adjacent to the DTB (arrows) or below the hypothalamus (closed arrowheads) in *cTKO* mice from E15.5-P0. K-L. NetrinG1-positive thalamocortical axons project from the thalamus and cross into the ventral telencephalon at the DTB (dashed line,

L) in close association with *Dlx5/6*-positive cells and axons (open arrowheads, L) at E13.5. M-N. In *cTKO* brains, thalamocortical axons have extended from the thalamus, however they have not crossed the DTB (dashed line, N). *Dlx5/6*-CIE cells and axons fail to span the DTB and remain positioned in the diencephalon (open arrowheads, N). Scale bars: scale bar in A represents 400 μm for A,B,F,G, 500 μm for C,D,H,I, and 600 μm for E,J; K,M 300 μm, 100 μm L,N.

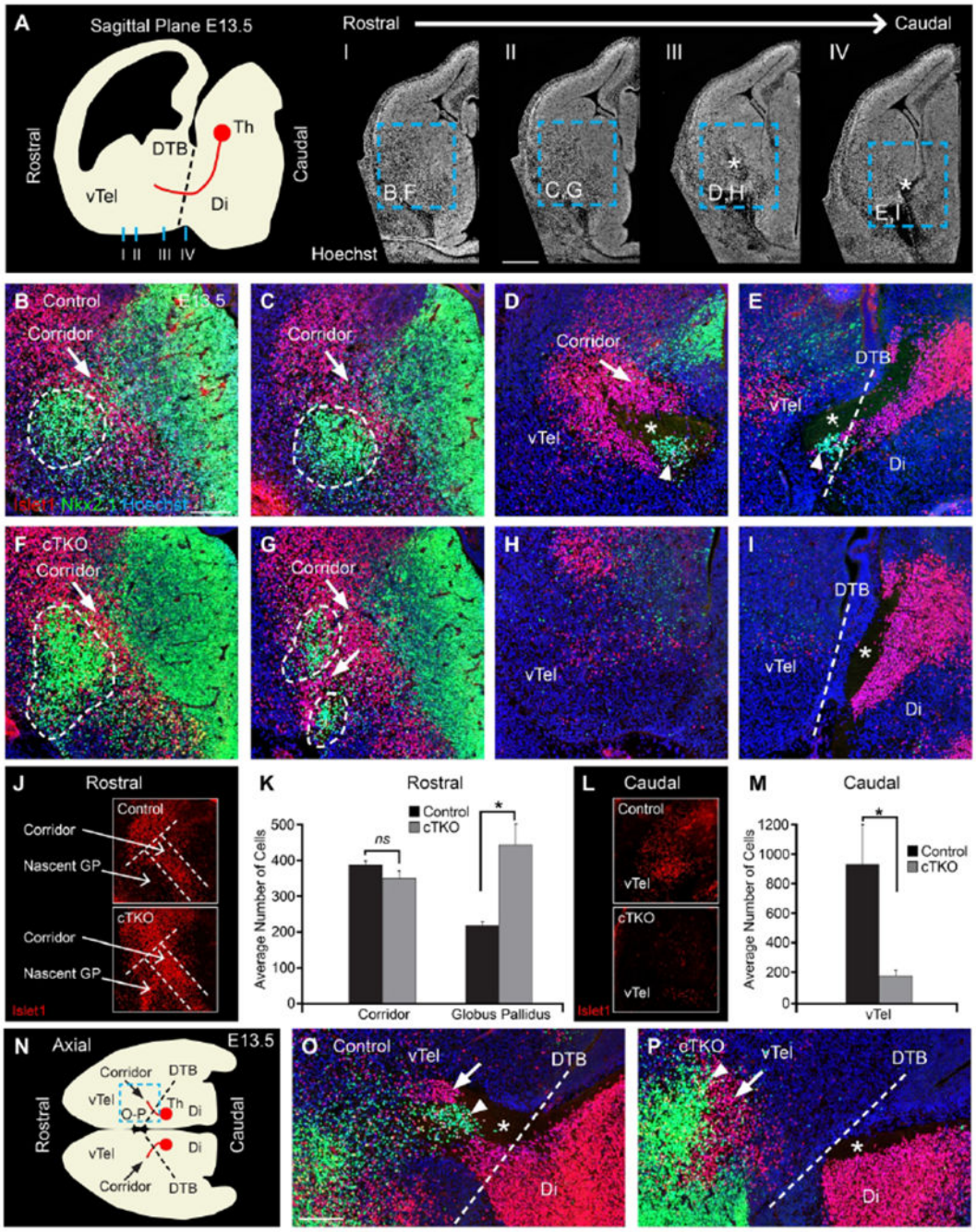

Figure 6. The ventral telencephalic corridor is malformed in *cTKO* brains at E13.5.

A. Schematic and Hoechst-labeled slices illustrating positions used for Islet1 and Nkx2.1 analysis. B-D. Islet1-positive cells (arrows) form a permissive corridor between the Nkx2.1-positive medial ganglionic eminence and globus pallidus (encircled B-C) through which unlabeled thalamocortical axons extend (asterisk, D). E. Thalamocortical axons (asterisk) cross the DTB (dashed line) above a patch of Nkx2.1-positive cells (closed arrowhead) and Islet1-positive cells from the diencephalon. F-I. In *cTKO* brains, the Islet1-positive corridor is present at rostral levels (arrows, F-G), but reduced at caudal levels (H-I). The

Nkx2.1-positive globus pallidus is expanded rostrally (encircled, F), ectopically infiltrated by Islet1-positive cells at mid levels (arrow, G), and diminished caudally (H-I) in *cTKO* brains. I. Thalamocortical axons (asterisk) fail to cross the DTB. Islet1-positive cells are present in the diencephalon, but are missing at the DTB (dashed line). J-M. Quantification of Islet-positive corridor cells at rostral (J-K) and caudal (L-M) levels. N-P. Axial view of the E13.5 corridor. Islet1- (arrows) and Nkx2.1- (closed arrowheads) positive cells extend caudally to where thalamocortical axons (asterisk) cross the DTB (dashed line) in controls (O), but stop rostrally in *cTKO* brains (P). vTel- ventral telencephalon, Di- diencephalon, DTB- diencephalon-telencephalon boundary. Scale bars: A 400 μm; B-I, N-P 150 μm.

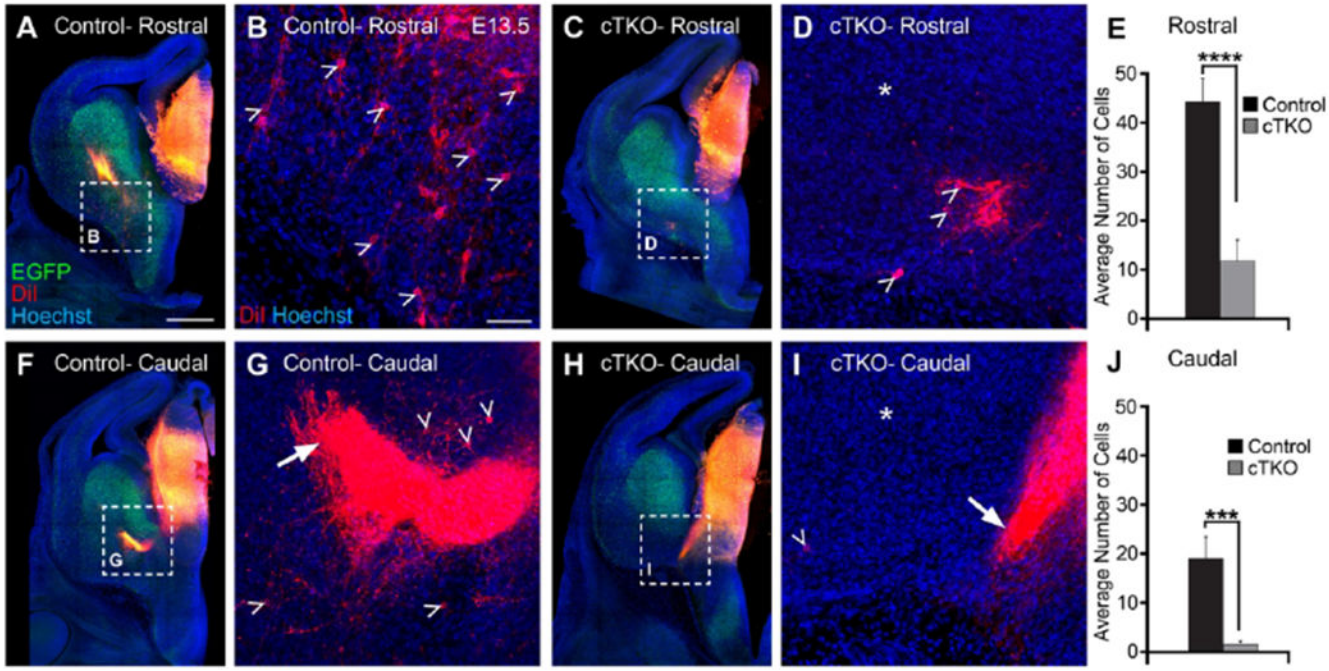

Figure 7. Ventral telencephalic guidepost cells are reduced in number in *cTKO* brains at E13.5.

A-E. After DiI placement in the dorsal thalamus at E13.5, retrogradely-labeled guidepost cells (open arrowheads, B,d) are present in the ventral telencephalon in control (A-B) and *cTKO* (C-D) brains, however are significantly reduced in number in the *cTKO* brain (E) at rostral levels. F-G. In control brains at caudal levels, both DiI-labeled thalamocortical axons (arrow, G) and retrogradely-labeled guidepost cells (open arrowheads, G) are present in the telencephalon. H-J. In *cTKO* brains, thalamocortical axons are missing in the telencephalon (asterisk, I), and instead project ventrally (arrow, I). A few retrogradely-labeled guidepost cells are present in the *cTKO* ventral telencephalon (open arrowhead, I), but are also significantly reduced in number (J) at caudal levels. Scale bars: A,C,F,H 400 μm, B,D,G,I 50 μm.

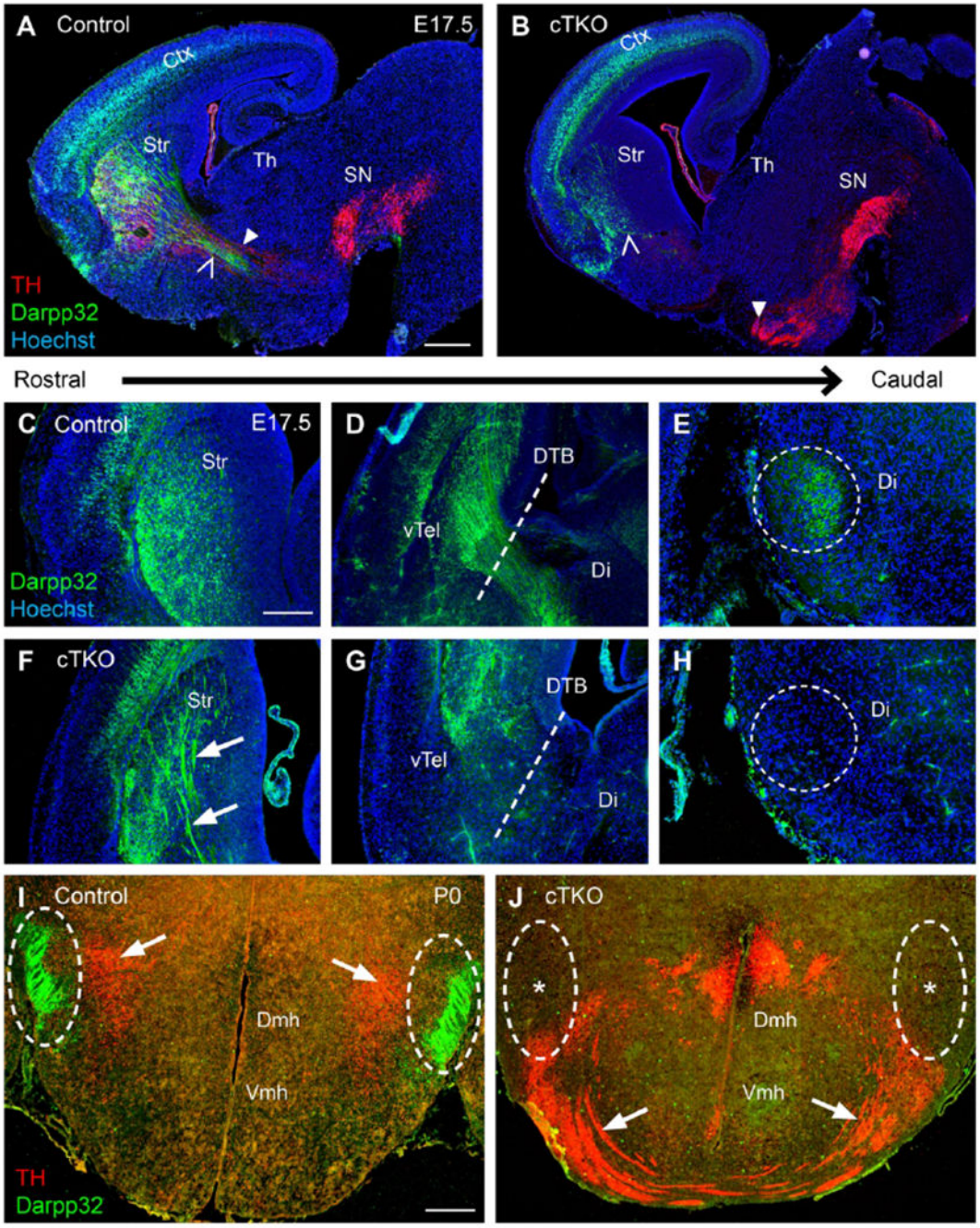

Figure 8. Axons fail to interconnect the striatum and the substantia nigra in *cTKO* brains.

A. In sagittal sections of E17.5 control brains, Darpp32-positive striatonigral axons (open arrowhead) and TH-positive nigrostriatal axons (closed arrowhead) project across the DTB in control brains. B. In E17.5 *cTKO* brains, Darpp32-postive axons (open arrowhead) fail to cross the DTB and TH-positive axons (closed arrowhead) misproject into the hypothalamus. C-E. In coronal sections of E17.5 control brains, Darrp32-positve axons are present in the striatum (C), cross the DTB (D), and reach the diencephalon (E). F-H. In E17.5 *cTKO* brains, Darrp32-positive axons are misrouted in the striatum (arrows, F), do not cross the

DTB (G), and are absent in the diencephalon (H). I. In coronal sections of P0 control brains, Darpp32 (encircled) and TH axons (arrows) travel adjacently in the hypothalamus. J. In P0 *cTKO* brains, Darpp32-positive axons are missing (asterisks), and TH-positive axons misroute ventrally (arrows). Ctx- cortex, Str- striatum, Th-thalamus, SN- substantia nigra, vTel- ventral telencephalon, Di- diencephalon, DTB- diencephalon-telencephalon boundary, Dmh- dorsomedial hypothalamic nucleus, Vmh- ventromedial hypothalamic nucleus. Scale bars: A-B, 400 μm; C-J, 250 μm.

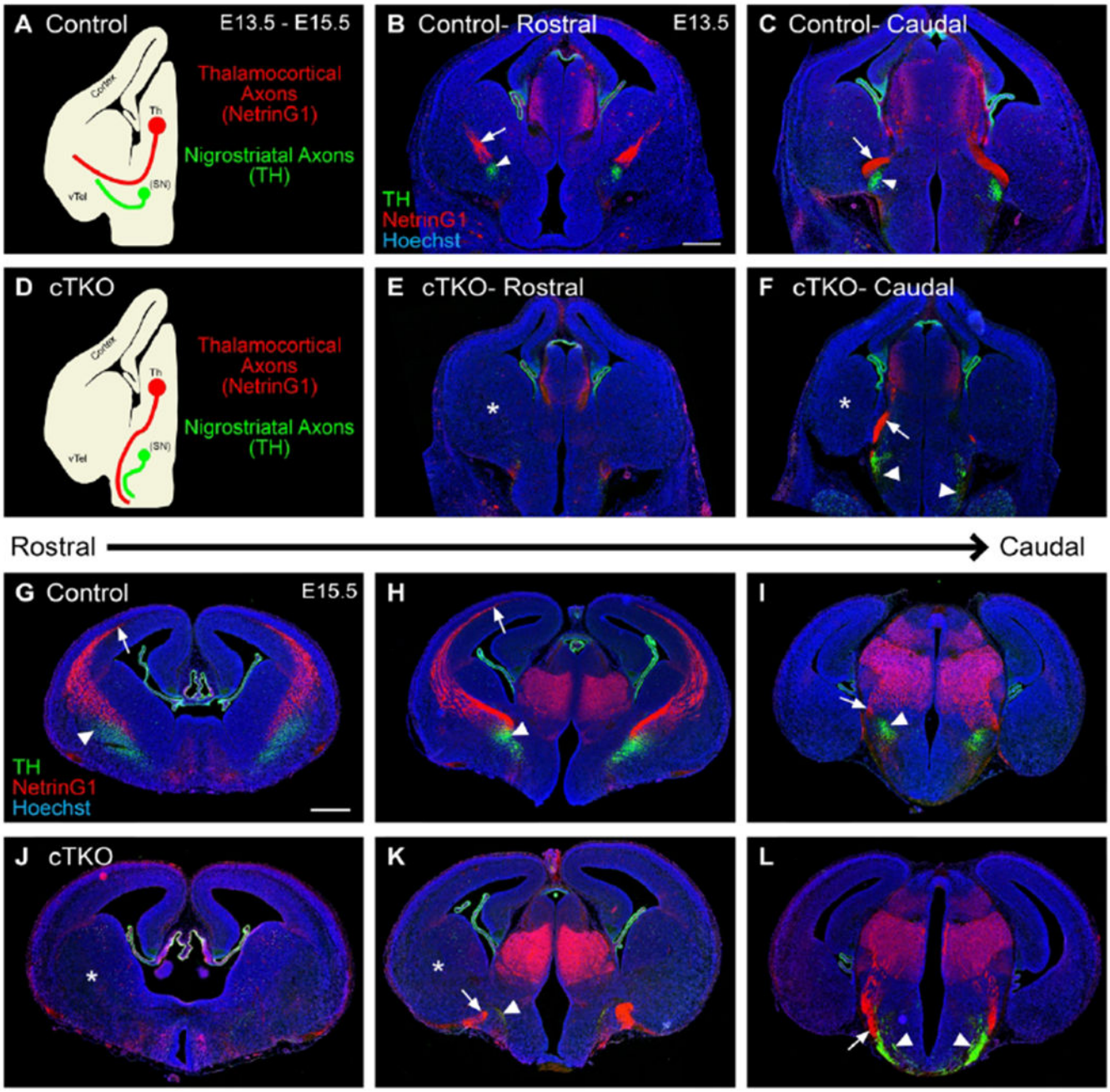

Figure 9. Nigrostriatal axons are misrouted in early development in *cTKO* mice.

A-C. In control brains at E13.5, NetrinG1-positive (red) thalamocortical axons (arrows) and TH-positive (green) nigrostriatal (closed arrowheads) axons cross the DTB and enter the telencephalon. D-F. In E13.5 *cTKO* brains, both thalamocortical and nigrostriatal axons fail to reach the telencephalon (asterisks). Nigrostriatal axons are misrouted at E13.5 in *cTKO* brains (closed arrowheads). G-I. At E15.5, NetrinG1 axons (arrows) reach the cortex, and TH (closed arrowhead) axons are present in the striatum in control mice. J-L. In *cTKO* brains at E15.5, both sets of axons fail to reach the striatum (asterisk), and NetrinG1

(arrows) and TH (closed arrowheads) mis-project ventrally. Th- thalamus, SN- substantia nigra, vTel- ventral telencephalon. Scale bars: B,C,E,F 400 μm, G-L 500 μm.

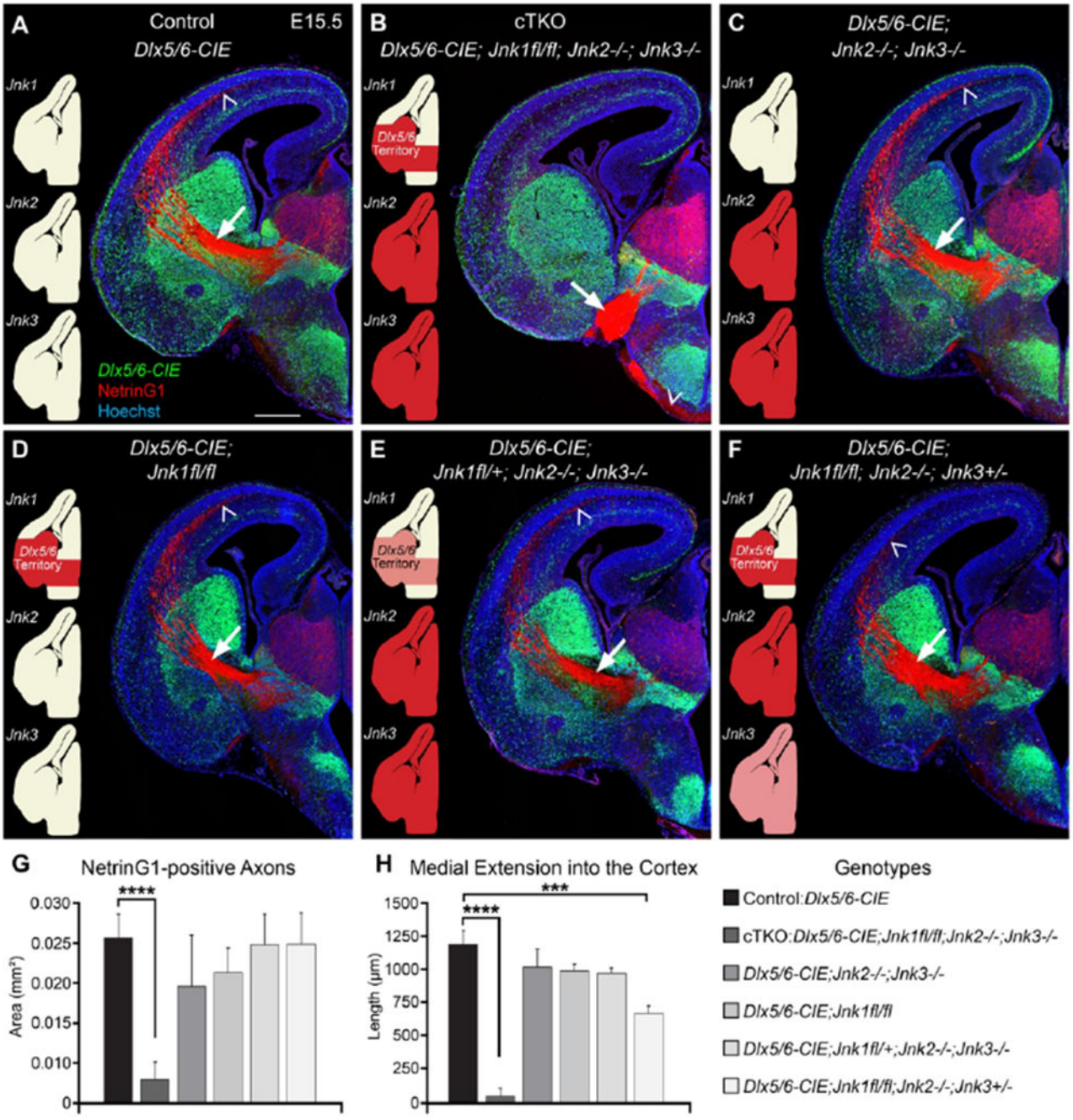

Figure 10. Thalamocortical axons require JNK signaling in the *Dlx5/6*-positive territory.

A. NetrinG1-labeled thalamocortical axons project through the *Dlx5/6*-positive ventral forebrain in the internal capsule (arrow) in route to the cortex (open arrowhead). B. In *cTKO* brains, NetrinG1-positive axons project to the ventromedial margin of the telencephalon (arrow) and extend into the hypothalamus (open arrowhead). C-F. NetrinG1-postive thalamocortical axons project through the internal capsule (arrows) and into the cortex (open arrowheads) in *Dlx5/6-CIE;Jnk2−/−;Jnk3−/−* (C), *Dlx5/6-CIE;Jnk1fl/fl* (D), *Dlx5/6-CIE;Jnk1fl/+;Jnk2−/−;Jnk3−/−* (E), and *Dlx5/6-CIE;Jnk1fl/fl;Jnk2−/−;Jnk3+/−* (F)

mice. G-H. Quantification of the abundance of NetrinG1-positive axons present at the entry zone of the cortex (G, one-way ANOVA $F(5, 30)=6.602$, $p= 0.0003$) and the medial extension of NetrinG1-positive axons into the cortical wall (H, one-way ANOVA $F(5, 30)= 39.63$, $p<0.0001$) at E15.5 in all genotypes. Asterisks in graphs indicate statistical significance determined by post-hoc Student's *t*-tests. In schematics, red indicates complete loss of a gene, while pink indicates one copy of the gene is deleted. Scale bar: 400 μm.

Table 1.

Offspring from experimental cross used to generate *cTKO* mice.

Age:	Litters:	Total Animals:	cTKO:	Percent:
E12.5	4	32	5	15.6% (5/32)
E13.5	19	149	19	12.8% (19/149)
E14.5	1	8	1	12.5% (1/8)
E15.5	31	208	28	13.5% (28/208)
E17.5	8	52	10	19.2% (10/52)
P0	33	216	30	13.9% (30/216)
P21	10	43	0	0.0% (0/43)

Numbers of litters, total animals, and *cTKO* mice recovered between embryonic (E) day 12.5 and postnatal (P) day 21. Expected ratios (1/8) of *cTKO* mice were collected at all time points except P21.